U.S. DEPARTMENT OF ENERGY | Office of ENERGY EFFICIENCY & RENEWABLE ENERGY

Chapter 07

Emerging Resources: Microalgae, Macroalgae, and Point-Source Carbon Dioxide Waste Streams

Table of Contents

7 Emerging Resources: Microalgae, Macroalgae, and Point-Source Carbon Dioxide Waste Streams

This report and supporting documentation, data, and analysis tools are available online:

- Report landing page: https://www.energy.gov/eere/bioenergy/2023-billion-ton-report-assessment-us-renewable-carbon-resources
- Data portal: https://bioenergykdf.ornl.gov/bt23-data-portal

7.1 Microalgae

Ryan Davis,[1] Andre Coleman,[2] Troy R. Hawkins,[3] Bruno Klein,[1] Jingyi Zhang,[3] Yunhua Zhu,[2] Song Gao,[2] Udayan Singh,[3] Longwen Ou,[3] Matthew Wiatrowski,[1] Lesley Snowden-Swan,[2] Peter Valdez,[2] and Yiling Xu[2]

[1] National Renewable Energy Laboratory
[2] Pacific Northwest National Laboratory
[3] Argonne National Laboratory

Suggested citation: Davis, R., A. Coleman, T. R. Hawkins, B. Klein, J. Zhang, Y. Zhu, S. Gao, et al. 2024. "Chapter 7.1: Microalgae." In *2023 Billion-Ton Report*. M. H. Langholtz (Lead). Oak Ridge, TN: Oak Ridge National Laboratory. doi: 10.23720/BT2023/2316175.

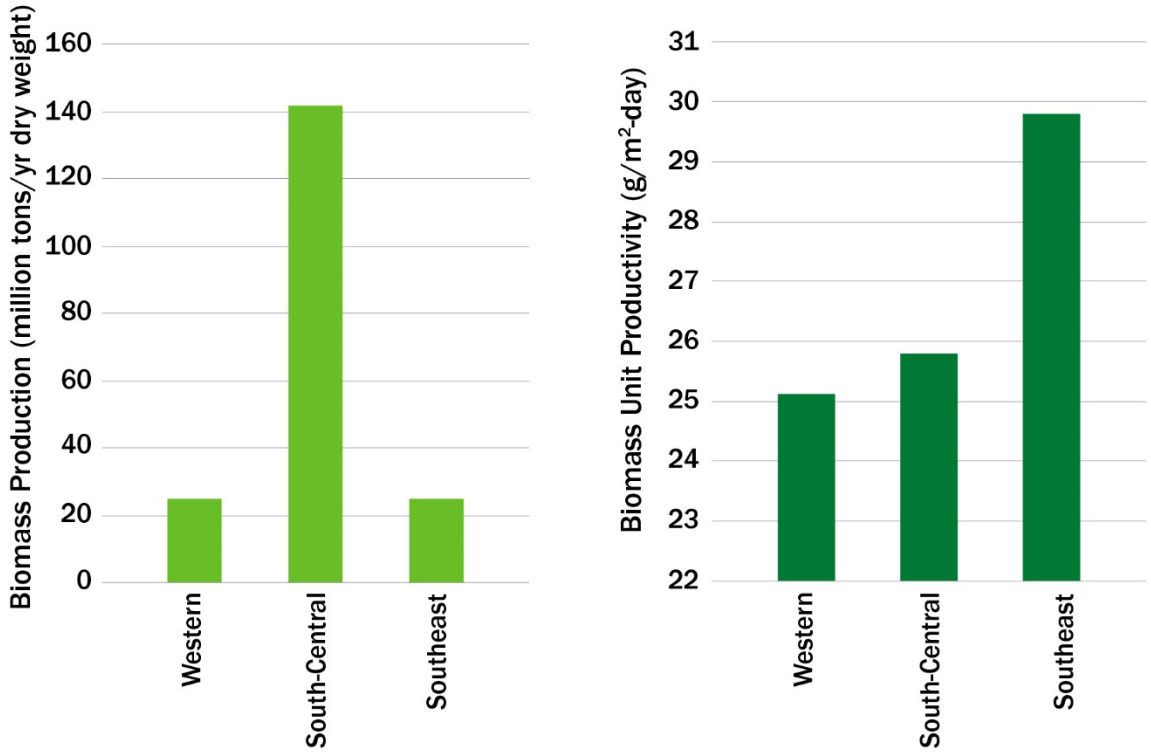

Figure 7.1. Total microalgal biomass and unit biomass productivity per region

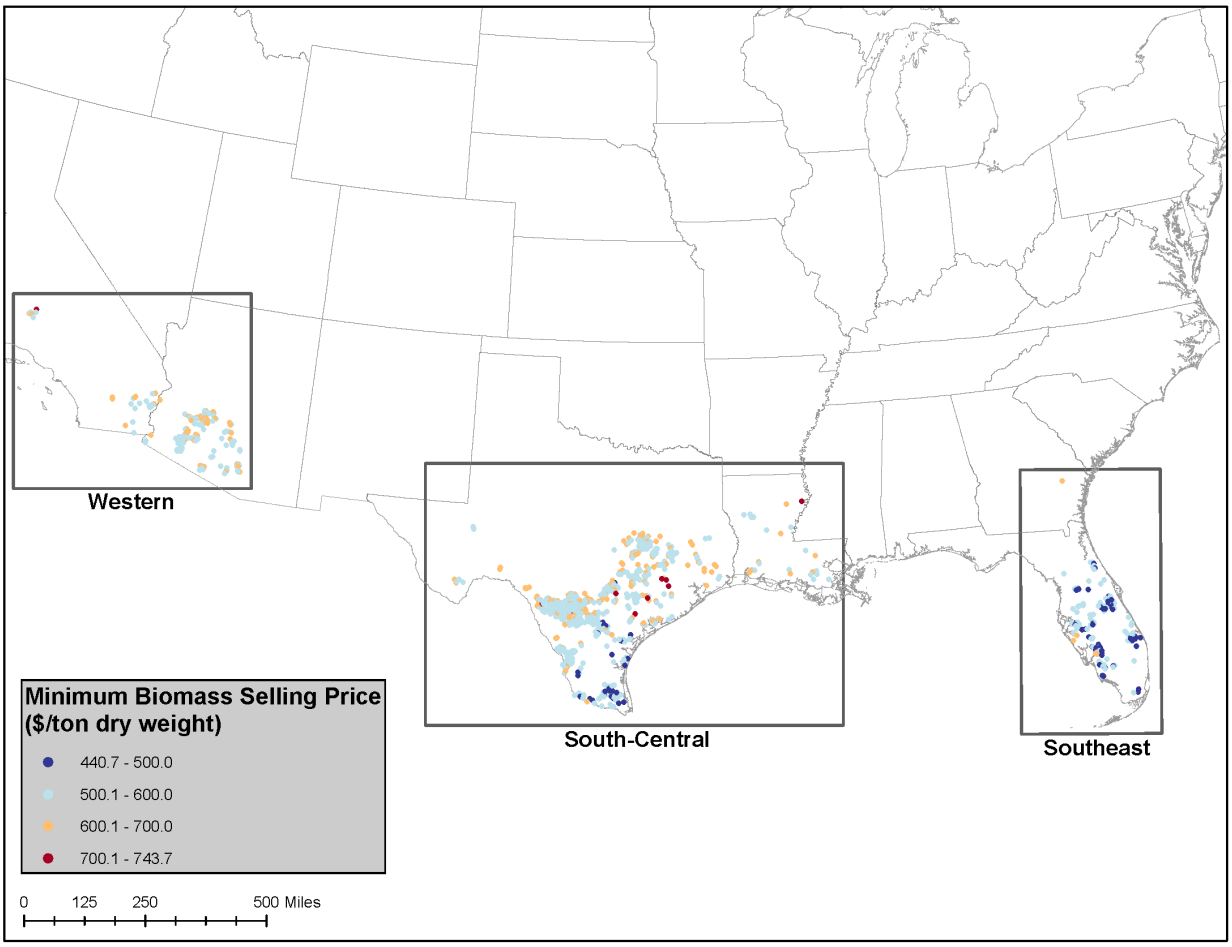

Figure 7.2. Spatial distribution of minimum biomass selling price (MBSP, 2020 dollars) by site and region

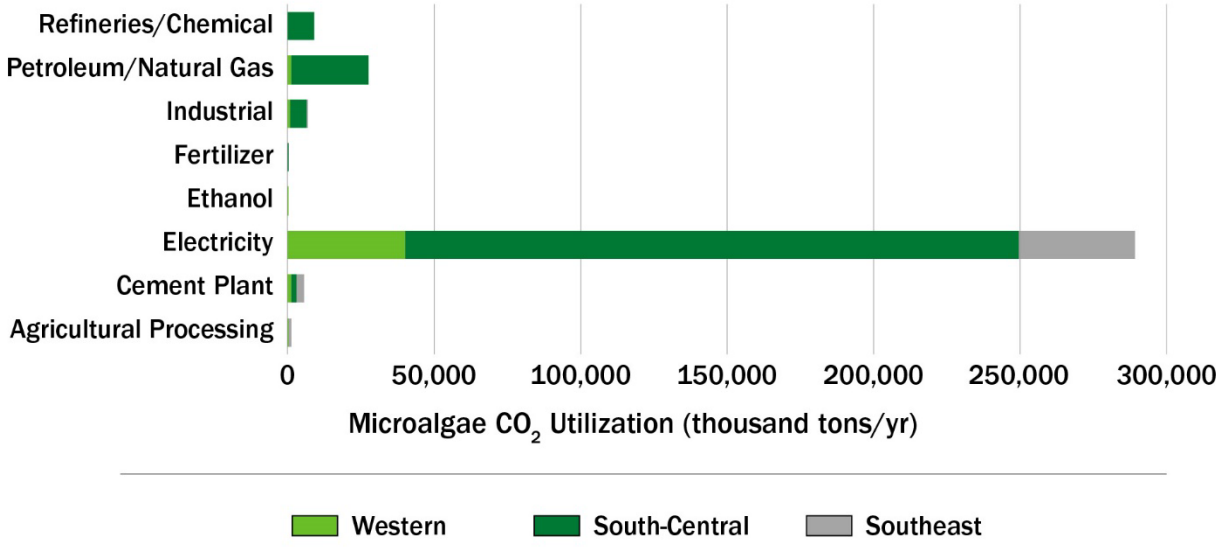

Figure 7.3. Source types and regional totals of waste CO_2 used for microalgae biomass production

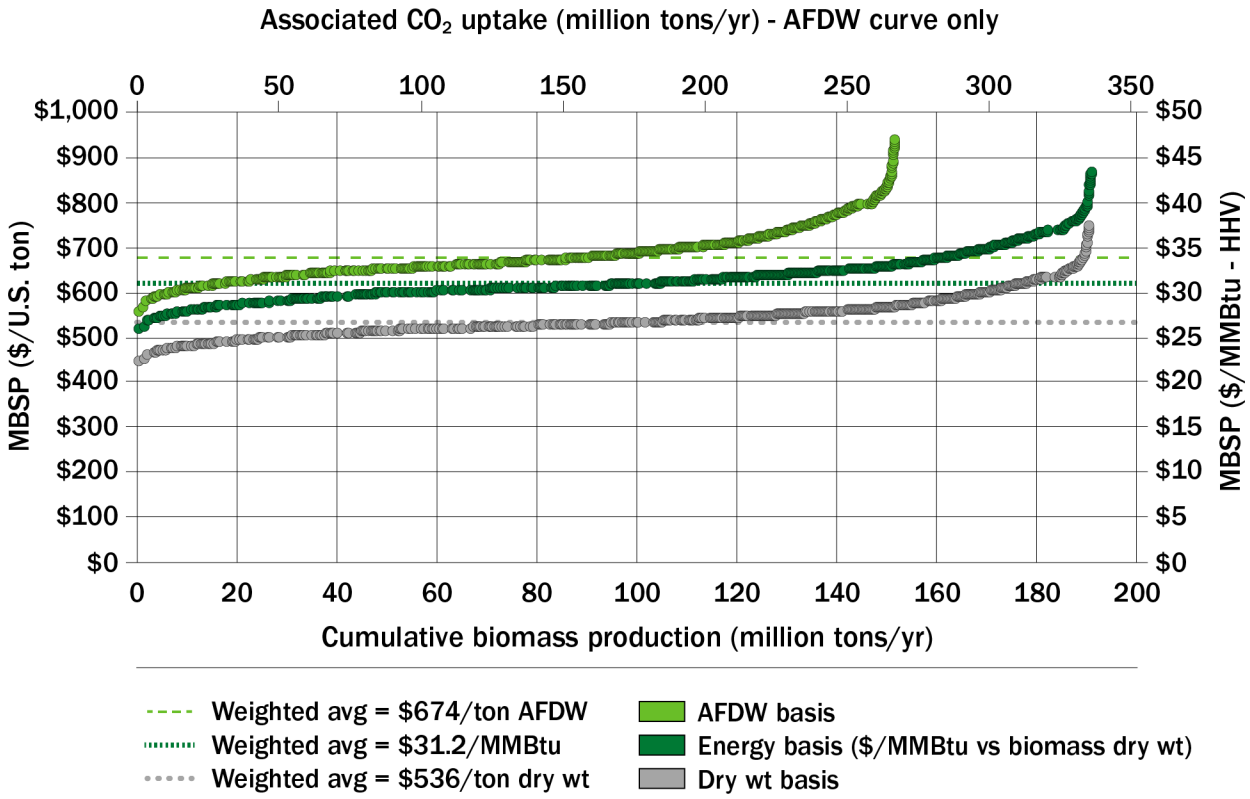

Figure 7.4. Supply curve of microalgae biomass (2020 dollars)

Summary

- Microalgae is a unique biomass resource that does not need to compete for land and water with other biomass feedstocks because it can be cultivated on low-quality unencumbered land using noncompetitive water types including saline and wastewater. It is included as a complementary resource alongside other biomass feedstocks reported in this study, albeit at higher biomass production costs reflective of more capital-intensive farming operations than typical for terrestrial biomass. Higher biomass costs can be offset by the potential to produce value-added coproducts unique to compositional constituents of microalgae.
- Relative to BT16, this chapter reflects the latest analysis from the *2022 Algae Harmonization Update*, which uses the latest parameterized and high-performing saline algal strain, second-generation carbon capture of point-source waste CO_2 and high-pressure pipeline transport resolved to specific point-source types, saline water sourcing up to 40,000 mg/L total dissolved solids for source and makeup water salinity, blowdown water treatment and recycle, and brine disposal handling.
- National-scale algal biomass availability potential was calculated at 152 million tons/yr ash-free dry weight (AFDW) (191 million tons/yr dry weight) at an average biomass

productivity of 26.2 g/m^2-day AFDW (about 50 tons/acre/yr dry weight).[1] The algal biomass was cultivated on 3.9 million acres of multi-criteria screened and potentially available land for CONUS and fixed 268 million tons of waste CO_2 based on biomass uptake.

- The algae biomass can be produced at an average MBSP of $674/ton AFDW ($536/ton dry weight) in 2020 dollars,[2] corresponding to a total energy potential of 3.3 quads/yr at an average MBSP of $31.2/MMBtu (higher-heating-value [HHV] basis).

7.1.1 Background

Introduction

Microalgae represents a source of biomass with a significant longer-term potential to meaningfully contribute to renewable fuels, chemical production, bioplastics, feeds, and more at the national scale and without direct competition with terrestrial biomass resources or food and feed agricultural production (Huntley et al. 2015; Zhu et al. 2020; Davis et al. 2018). The benefits of microalgae as a complementary biomass resource are well documented in literature, including (1) the ability to utilize non-arable or otherwise unencumbered land for open-pond or closed-photobioreactor cultivation systems; (2) the ability to grow in generally noncompetitive water including brackish, saline, or other non-freshwater media such as wastewater; (3) significantly higher growth rates and associated land use efficiency (i.e., high-density biomass per unit land area) for biomass production compared to terrestrial biomass sources; (4) unique compositional characteristics of algal biomass that allow for numerous conversion options to various fuels and/or value-added products; and (5) typically high biomass carbon to energy content and associated CO_2 uptake potential (Brennan and Owende 2010; Miara et al. 2014; Huntley et al. 2015; Bleakley and Hayes 2017). Generally speaking, microalgae require a CO_2 uptake ratio of approximately 2 tons CO_2 per ton of produced biomass (Judd et al. 2015); for this analysis, high-rate production of the saline strain algae used under nutrient-replete conditions fixes about 1.76 tons CO_2 for every ton of biomass, translating to 268 million tons/yr of point-source waste CO_2 utilized. This result is based on biomass uptake alone and excludes an additional 72 million tons/yr CO_2 reflecting capture and transport efficiencies and subsequent rerelease of CO_2 through outgassing from the ponds at a 75% CO_2 utilization efficiency targeted in the analysis. Use of sparged, concentrated CO_2 (typically piped in from point-source carbon capture) is generally required to sustain high growth rates required for economic viability, although direct air capture systems are also being researched.

Owing to costs of biomass cultivation currently being roughly an order of magnitude higher than for conventional terrestrial energy crop sources, microalgae is generally viewed as a future available resource in the context of producing economically viable commodity energy products such as renewable diesel and SAF, relative to some other biomass feedstocks discussed in this report (Reed et al. 2023). Microalgae feedstocks have demonstrated flexibility in producing end-

[1] In Section 7.1, "tons" refers to U.S. tons.
[2] In Section 7.1, all costs are in 2020 dollars.

use products, including energy products (i.e., renewable diesel, naphtha, bioethanol, biokerosene and aviation fuels, biobutanol, and biomethanol), with the most straightforward and commercially practical approach to extract and upgrade algal lipids to renewable diesel and SAF through the commercial hydroprocessed esters and fatty acids (HEFA) pathway. In spite of the high cost for microalgae biomass, the high energy content of this feedstock can enable very high fuel yield potential—more than 120 gallons of gasoline equivalent (GGE) per ton of biomass—compared to terrestrial feedstocks, typically on the order of 40–80 GGE/ton (Davis et al. 2014; Jones et al. 2014). Numerous non-energy products can also be made from microalgae, including bioplastics, pigments, nutraceuticals, omega-3 fatty acids, carotenoids, biofertilizer, cooking oils and food products, and feeds for aquaculture, poultry, and livestock (Devi et al. 1981; García, De Vicente, and Galán 2017; Caporgno and Mathys 2018; Molino et al. 2018; Laurens et al. 2017).

Currently, the microalgae industry in the United States is small, at <500 acres based on dedicated algae farms (not considering algae-based remediation at wastewater treatment plants). Under current commercial operations not associated with wastewater remediation, microalgae cultivation is largely focused on very high-value, small-volume food and nutraceutical products such as omega-3 fatty acids, supplements, and carotenoids. Beyond pilot experimental operations, algae is not currently produced for fuel production at commercial scale today. Outside the United States, a larger commercial microalgae industry exists primarily for food and aquaculture products, with a total global production volume of roughly 60,000 tons/yr, concentrated primarily in Asia (Cai et al. 2021; FAO 2021). Beyond the high-value market, microalgae may hold more near-term potential in co-benefit economical fuels production via low-cost “waste” resources such as collection of harmful algal blooms in water bodies and direct utilization in municipal and industrial wastewater treatment for nitrogen, phosphorus, and heavy metal mediation (Wiatrowski et al. 2022), although this is limited to a smaller overall resource potential (likely no more than 28 million tons/yr national-scale biomass potential, compared to dedicated algae farming on the order of 150 million tons/yr, as is the focus of this chapter) (Clippinger and Davis 2021; Wiatrowski et al. 2022).

This chapter summarizes the latest microalgae analysis work conducted by DOE national laboratory partners Pacific Northwest National Laboratory, NREL, and Argonne National Laboratory, focused on a 2022 algae model harmonization analysis spanning resource assessment, techno-economic analysis (TEA), and life cycle analysis, respectively, for future microalgae production performance envisioned via dedicated high-rate, open-pond microalgae farming (Davis et al. 2024). This analysis is conducted across 980 individual locations, which by the nature of a land and resource screening analysis vary in area for an individual algal farm ranging between 1,000 and 39,000 acres (average farm size of 3,940 acres). These individual farms are modeled and then collated into an overall national-scale biomass potential spanning the full collection of identified suitable farm locations. This work builds from a prior harmonization study conducted with the same national laboratory partners in 2017 (published in 2018) that followed a similar framework spanning resource, economic, and sustainability assessment for national-scale algal systems but under a different set of assumptions and less model granularity

(Davis et al. 2018). Relative to BT16's microalgae chapter (Langholtz, Stokes, and Eaton 2016) and the subsequent 2017 harmonization study, the analysis conducted for the 2022 model harmonization update, and summarized here for BT23, reflects a number of key updates and modifications:

- Land suitability analysis was revised using latest available land use/land cover data and protected and sensitive areas, and further excludes areas with high primary productivity to avoid disturbance of natural carbon capture and storage. Relative to BT16, the updated analysis includes 115% of the land area (3.86 million acres) producing 335% of the annual biomass (191 million tons/yr dry weight). The noted increases are largely due to the use of next-generation carbon capture and transport, noted next.
- CO_2 sourcing is handled via modeling second-generation carbon capture and utilization from a variety of nearby waste CO_2 point sources. The modeled high-purity captured CO_2 is transported over high-pressure pipelines, greatly increasing the distance that CO_2 can be economically delivered to potential algae cultivation sites. This increases the total amount of biomass production potential relative to the transport of single-source-type bulk flue gas through large-diameter pipelines to collocated algae farms (as assumed in BT16).
- Variable-scale cultivation farms ranging from a minimum area of 1,000 acres to a maximum of 39,000 acres of production pond area are used to align with the total CO_2 and water resource availability in a localized area (average size of the full collection is 3,940 acres, versus fixed farm scales at 5,000 acres in the 2017 harmonization study or 1,000 acres in BT16).
- Consideration was given only for saline algae cultivation (no freshwater scenario included), utilizing a high-salinity-tolerant strain (approximately 50,000 mg/L) deployed under DOE's Development of Integrated Screening, Cultivar Optimization, and Verification Research (DISCOVR) consortium (Huesemann et al. 2023) to maximize productivity, minimize contamination, and reduce competition for freshwater resources.
- Relative to the 2017 harmonization, further granularity is now included regarding the cost and energy demand for second-generation CO_2 capture based on the specific point-source flue gas concentration, site-specific saline water sourcing, pond water blowdown management, forward osmosis treatment of pond blowdown water including freshwater recycling (utilized for washing dewatered biomass to reduce salt content, as well as recycle to the ponds), and disposal of remaining brine volume via deep-well injection.
- Cultivation and harvesting are performed under more nutrient-replete conditions, yielding biomass with higher protein and lower lipid/carbohydrate content. Although this is generally a less favorable composition for purposes of downstream conversion to fuels, it represents a more readily achievable composition to achieve cultivation productivity targets in the nearer term (slightly exceeding BETO's 25-g/m^2/day productivity target [BETO

2020] at 26.2 g/m^2/day over the full collection of sites) and may allow for coproduction of protein for food and feed markets (outside the scope of this chapter).

7.1.2 Methods Summary

The model and information flows for microalgae biomass in BT23 are depicted in Figure 7.5, focusing on the Biomass Assessment Tool (BAT) resource assessment flows and the algae farm TEA model elements to the point of ready-to-use biomass. A detailed schematic of the TEA model is presented in Figure 7.6.

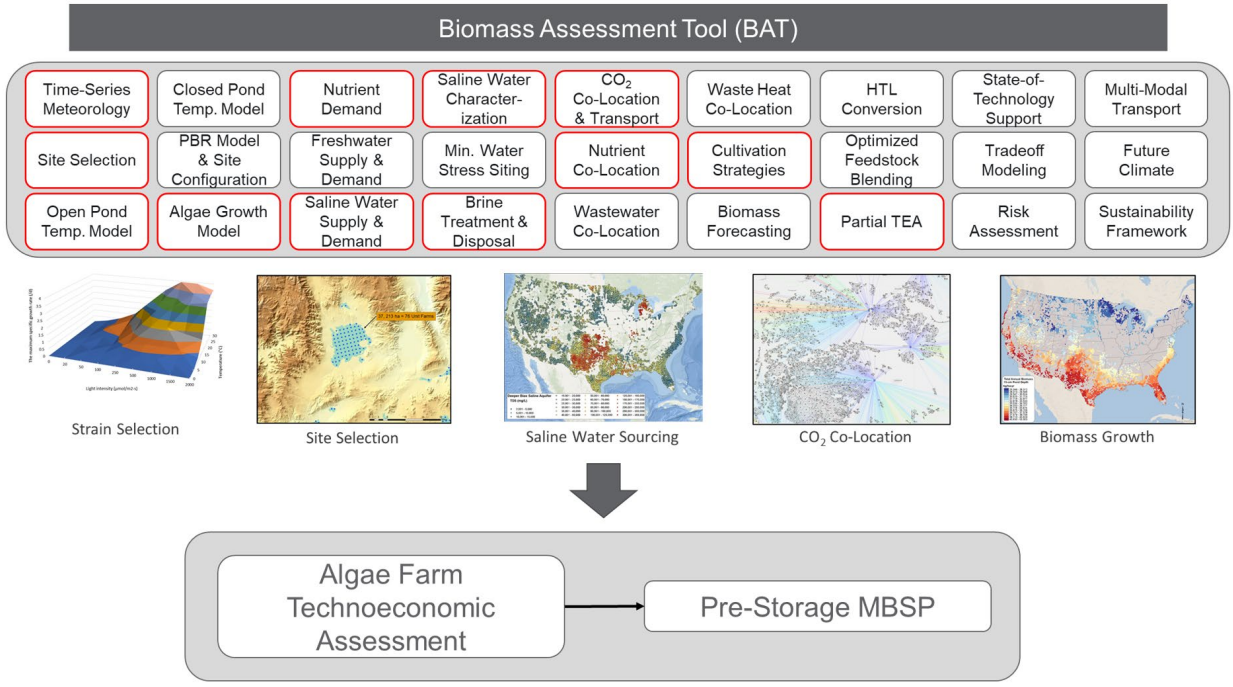

Figure 7.5. Components and workflow for microalgae resource analysis and TEA for BT23. The red highlighted boxes indicate the BAT modules used in this assessment.

Resource Analysis

BAT is a resource assessment and partial techno-economic modeling system comprising numerous modules that combine multiscale spatiotemporal modeling, biophysical modeling, and resource demand and availability using the best-available climate, water, land, and infrastructure data, along with environmental constraints, biomass growth parameterization, and more (Coleman et al. 2014; Venteris et al. 2014; Wigmosta et al. 2017; Sun et al. 2020; Xu et al. 2020; Ou et al. 2021).

A 2022 updated CONUS-wide, multi-criteria land screening model was used to identify potential open-pond algae cultivation sites in the CONUS, with exclusions of steep topography, land use restrictions, existing cultivated agriculture, forestlands, wetland, riparian areas, areas with high net primary productivity (carbon storage), and other environmentally sensitive areas (see the appendix for details).[3] We assume that a 1,000-acre contiguous land area is the minimum to be

[3] Access BT23 appendices at www.energy.gov/eere/2023-billion-ton-report.html.

included as a single farm, and the model does not enforce a maximum area threshold. The resulting contiguous land area for any given farm location is translated to the algae farm TEA model scaled to the same size, resulting in 3,255 individual sites that have variable algae farm areas from 1,000 to nearly 39,000 acres in size (averaging 3,940 acres across the full collection). The variable areas reflect how these systems could be deployed to maximize available economies of scale based on local resource availabilities and integration with downstream conversion facilities (outside the scope of discussion in this chapter).

For this analysis, potential cultivation sites are further constrained by (1) the availability of nearby, non-committed waste point-source CO_2 that can be captured and transported to the site for ≤$82.67 ton (≤$75 tonne); (2) availability of saline groundwater resources at a salinity between 2,000 and 40,000 mg/L at depths <500 m; and (3) a long-term mean daily algal biomass productivity of ≥25 g/m^2-day, resulting in 1,199 remaining sites. These sites are further downselected to 980 sites in the TEA process when limited to a $1,000/ton MBSP threshold. As a means of easily distinguishing sites based on location, the unit farms are organized into three regional groupings spanning the Western, South-Central, and Southeast CONUS regions (Figure 7.7). Note that the regional groupings are not used in the algae farm TEA models, as all biomass costs are calculated on an individual farm basis to best reflect site-specific conditions.

A high-performing saline strain investigated under the DISCOVR project was used in this assessment: *Tetraselmis striata* LANL 1001 (Huesemann et al. 2023). Using the Microalgae Growth Model within the BAT, algae biomass production was simulated for each screened site in the CONUS using 40 years of hourly meteorological data, including air temperature, relative humidity, precipitation, wind speed, atmospheric pressure, and solar radiation components. The growth rate of *Tetraselmis striata* LANL 1001 was modeled as a function of light intensity and temperature under nutrient-replete conditions. Thus, the local meteorology and long-term climatology directly impact the productivity potential. In combination with the land screening, available saline groundwater, and collocated, economically viable CO_2 location and transport, this impacts where the farm sites are located. The resulting growth model output provides a site-specific cumulative monthly time-series, total unit area biomass output (kg/ha) (Huesemann et al. 2013). No additional biomass scaling was performed here as was done in the future-looking microalgae scenarios under BT16 (Langholtz, Stokes, and Eaton 2016). Microalgae are assumed to be harvested when algae reach 0.05 wt % (0.5 g/L) concentration.

Utilizing the BAT CO_2 capture and transport module, a location-based demand and allocation spatial network model, we use the location-specific biomass productivity to establish a daily carbon demand, the 2020 reported annual point-source emissions, and the source type, subsequent CO_2 purity, and specific location. Without site-specific, time-varying operational details from the annual reported CO_2 emissions, we assume an equal daily mass availability of CO_2, and the transport pipeline calculations are established based on distance, available CO_2 mass, and the ability to hold 8 hours of additional CO_2 overnight, a process known as line packing. The model assumes that 90% of the reported emissions are captured using second-

generation carbon capture and utilization, and the biomass CO_2 utilization efficiency is established at 75%, closely patterned after Huntley et al. (2015). Individual point-source CO_2 sites are able to effectively supply one to many cultivation sites, until the CO_2 supply is exhausted or exceeds the specified cost threshold, which for this study is defined as $82.67/ton ($75/tonne). Direct air capture systems were not considered here, as the cost and energetics models have not yet been built into the BAT or TEA models. Additional CO_2 modeling parameters can be found in the harmonization report (Davis et al. 2024). The BAT open-pond temperature model was established with saline operating conditions to a threshold salinity of 55,000 mg/L, reflecting the lab testing conditions in which *Tetraselmis striata* LANL 1001 was parameterized. The pond model provides a mass balance for the incoming site-specific groundwater source salinity and mass density/volume for the pond area and managed depth, and considers incoming precipitation, salinity, and temperature-based evaporative losses, as well as blowdown water volume required to maintain pond threshold salinity. The blowdown water volume is processed through a forward osmosis system, where at about 55,000 mg/L total dissolved solids, 82% of the blowdown volume is recovered as freshwater, and the remaining 12% volume is disposed of through deep-well injection. The recovered freshwater is directed first for use downstream to wash the dewatered solids to reduce salt concentrations to 15,000 mg/L, and with remaining freshwater is recycled to the ponds when available. The blowdown water volume removed from the pond is replaced with makeup water, sourced first from the forward osmosis processed water, if available, then from the saline groundwater well as required.

Algae Farm TEA

The outputs from the BAT model are run through NREL's algae farm TEA model, largely based on the set of operations and assumptions in NREL's 2016 algae farm design report (Davis et al. 2016) and the more recent 2017 harmonization report (Davis et al. 2018). Key updates were made to the published model framework for this study, including (1) incorporation of wet anaerobic storage to mitigate seasonal variabilities based on recent performance data from Idaho National Laboratory (Klein and Davis 2022) (biomass costs are tracked both before and after seasonal storage); (2) addition of a basket strainer and wash water step during dewatering to reduce exogenous ash and salt content, respectively, for downstream conversion equipment protection (using freshwater recovered from forward osmosis); and (3) inclusion of forward osmosis and updated injection well costs/power demands from the BAT models for handling saline blowdown water. In order to avoid any external freshwater usage in the algae farm/dewatering operations, if more freshwater is required for the washing step than is available from the forward osmosis unit, additional saline water is routed to the forward osmosis unit until necessary freshwater volumes are achieved (increasing costs for forward osmosis and saline injection disposal, but at the avoidance of externally sourced freshwater as an important priority for saline cultivation).

All capital and operational costing are updated to 2020 dollars, and capital expenses are designed around maximum seasonal productivities, while variable operational expenses are based on monthly resource use and throughputs. Site development and operational costs, including pond

construction and circulation systems, inoculation train, groundwater source well(s), forward osmosis system, brine injection wells, CO_2 storage and delivery (following off-site capture and pipeline transport to the farm gate), nutrients, dewatering systems, and other site development costs, are included as depicted in Figure 7.6. Additional TEA modeling details can be found in the harmonization report (Davis et al. 2024) and Davis et al. (2016, 2018).

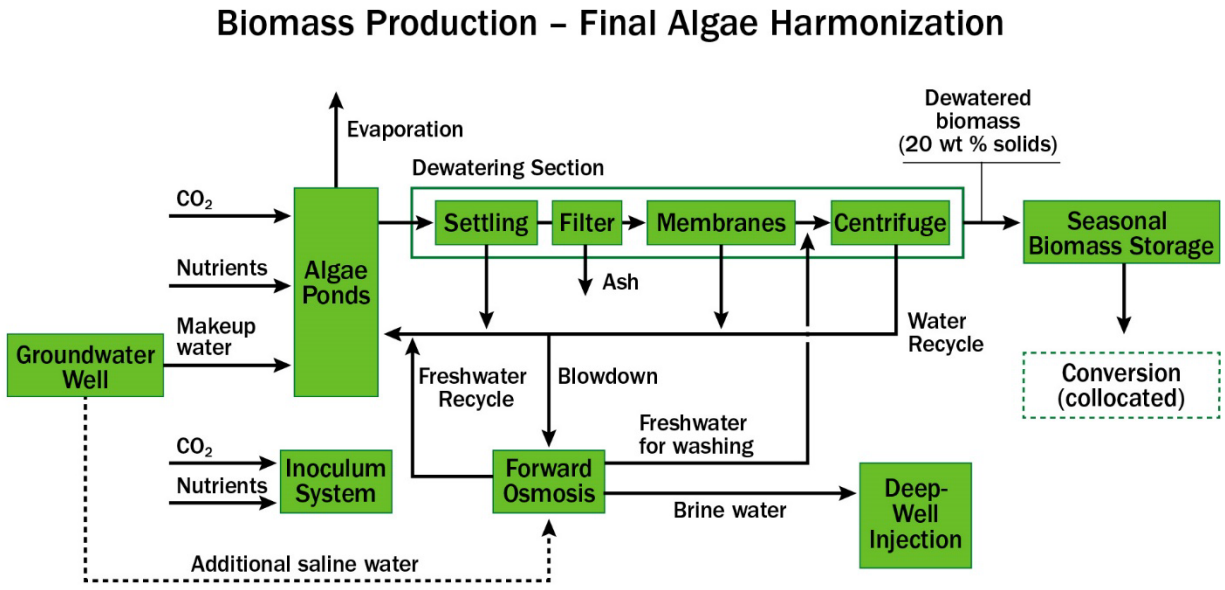

Figure 7.6. Site-level algae farm techno-economic framework used in this study, from cultivation to harvesting and seasonal biomass storage

7.1.3 Results

The location siting analysis and associated TEA analysis cutoffs ultimately identified 980 independent and contiguous potential algae cultivation sites covering a total pond area of 3,858,226 acres (1,561,368 ha). The sites dominate across five Southern-tier states, including Texas (2.85 million acres), Florida (433,000 acres), Arizona (452,000 acres), Louisiana (51,000 acres), and California (70,000 acres). The 40-year long-term daily productivity mean across all sites is 26.2 g/m^2-day (49.5 tons/acre-yr dry weight), achieving the 2030 BETO goal of 25 g/m^2-day, and summing to a total of 151.9 million tons/yr of AFDW biomass (190.9 million tons/yr dry weight) (Figure 7.9). Biomass productivities and associated costs are reported by region (Figure 7.7, Figure 7.8, and Table 7.2) and by individual farm (Figure 7.10 and Figure 7.11), with accompanying data including county-level and state-level designations so data can be evaluated in multiple ways.

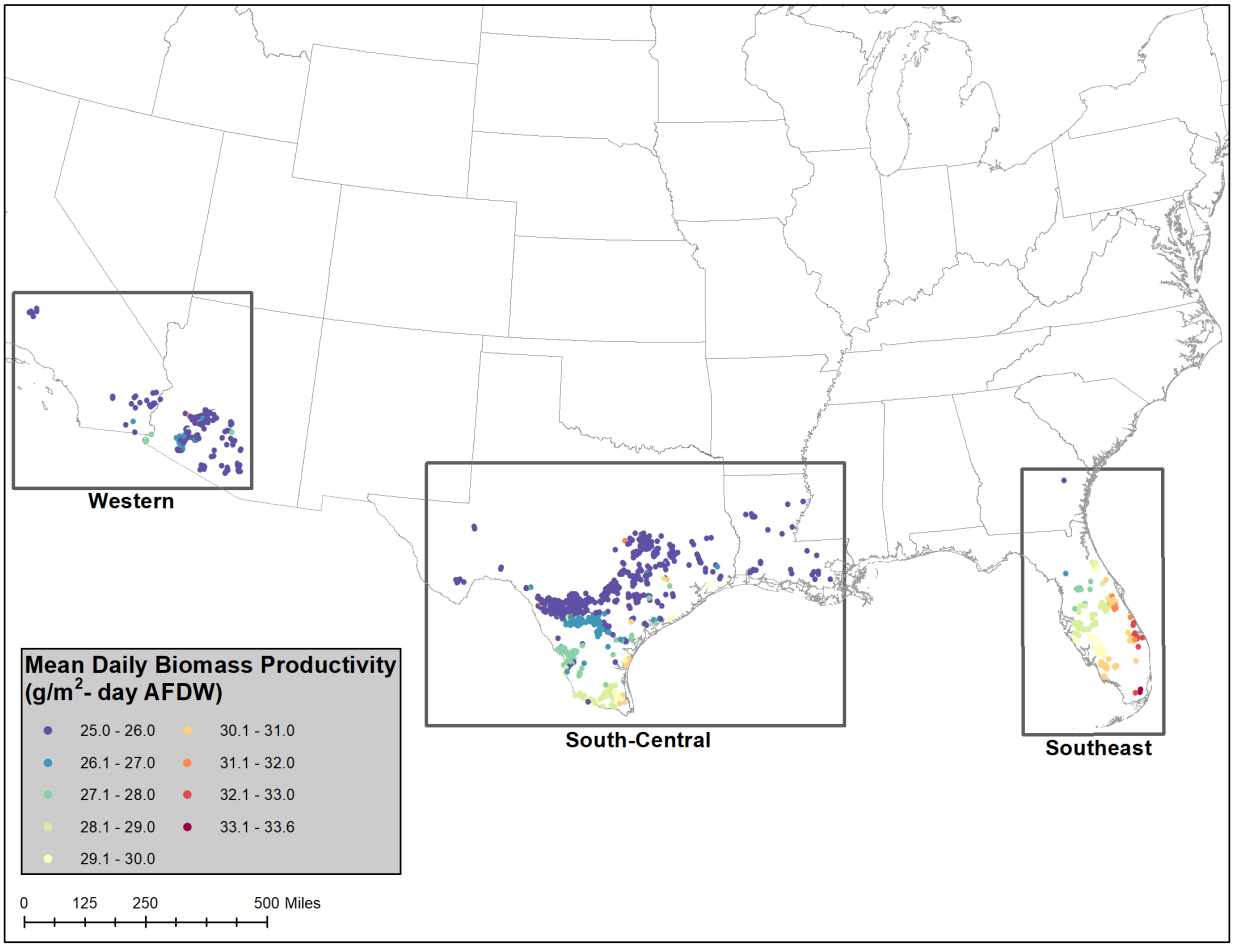

Figure 7.7. Targeted long-term mean daily biomass productivity (g/m²-day AFDW) for potential microalgae cultivation sites. The collection of individual sites is organized into regional groupings for reporting purposes.

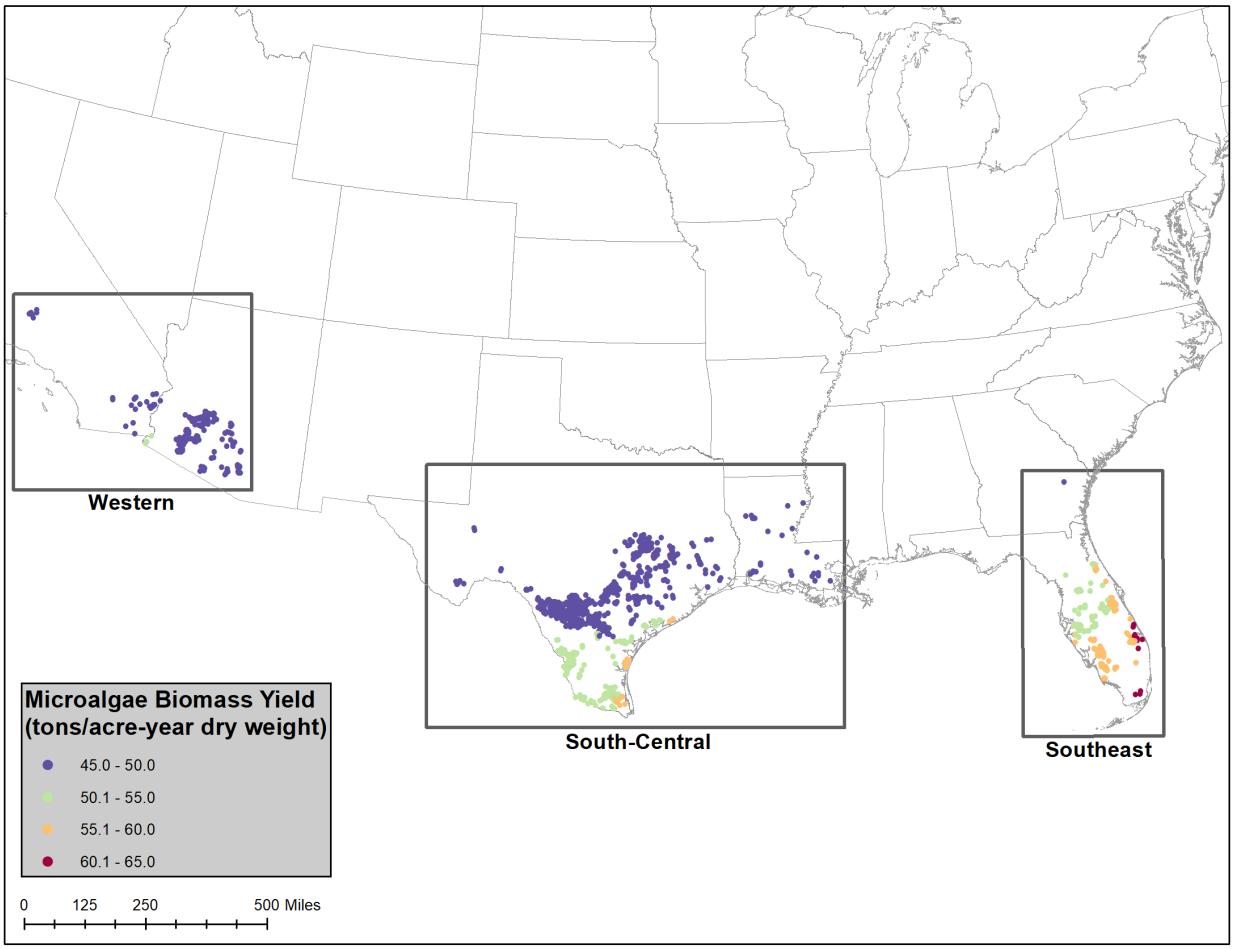

Figure 7.8. Site-scale annual microalgae biomass yield (tons/acre-year dry weight)

An important consideration in high-productivity algae cultivation is the access and utilization of CO_2, which is key for not only increasing productivity, but also meeting reduced GHG and carbon intensity targets. We assume here that 90% of 2020 reported annual CO_2 emissions (not CO_2e) are captured at the point source and transported to one or many cultivation sites, depending on the waste resource availability, total algae farm demand, and spatial proximity to economically transport CO_2 over high-pressure pipeline (Song et al. 2018). Further, we assume a 75% CO_2 uptake efficiency by the algae, with the remaining 25% delivered into the ponds, ultimately being outgassed or otherwise not used (Huntley et al. 2015). In total across all site groups, 170 point-source waste CO_2 sites are used to capture and transport 340 million tons/yr of CO_2 for algae cultivation (11.02% of CONUS total waste CO_2). On average, across all 980 potential algae cultivation sites, CO_2 is transported 23.32 miles by high-pressure pipeline. The collocated point-source waste CO_2 locations and source types are varied regionally. Table 7.1 provides a high-level assessment of CO_2 utilized for algae cultivation with respect to regional availability across the CONUS. While the algae cultivation sites are limited to Southern-tier states (Figure 7.7), to better gain a CONUS-perspective, the algae "Western" region is expanded to the 11 Western states (including and west of Montana, Wyoming, Colorado, and New

Mexico); the algae "South-Central" is expanded to "Central" and includes 13 states east of the defined Western states and those west of the Mississippi River from Wisconsin to Louisiana; and "Southeast" is expanded to "East," including the remaining 25 states east of the Mississippi River. As modeled here, approximately 15.0% of the U.S. national waste CO_2 can be beneficially utilized by microalgae processes, and approximately 9.6% of the national waste CO_2 total is fixed in the microalgae biomass. While the scope of this work was limited to current non-biogenic point-source CO_2 availabilities today, as industrial decarbonization progresses, this availability may become more limited moving into the future. Under such a scenario, to maintain (or increase) the total algal biomass potential, alternative sources of CO_2 would need to be brought in. This could include biogenic CO_2 as may be available from other terrestrial biomass processing operations if projections in the billion-ton study are realized, and/or incorporate direct air capture to decouple entirely from point-source reliance.

Table 7.1. Simulation Results for CO_2 Source Types by CONUS Region, Total CO_2 Used for Microalgae (thousand tons/yr), and the Number of Facilities Used

CO_2 Source	West		Central		East	
	Thousand tons CO_2/yr [% of regional]	# sites [% of regional]	Thousand tons CO_2/yr [% of regional]	# sites [% of regional]	Thousand tons CO_2/yr [% of regional]	# sites [% of regional]
Agricultural processing	353.8	8	0	0	401.9	5
	[7.1%]	[10.1%]	[0%]	[0%]	[5.0%]	[4.0%]
Cement plant	3,629.1	4	6,258.3	10	1,081.8	3
	[19.3%]	[9.5%]	[17.5%]	[21.3%]	[2.6%]	3.5%
Electricity generation	39,725.0	33	209,318.5	67	71,826.2	39
	[12.5%]	[11.0%]	[74.1%]	[14.8%]	[6.6%]	[5.8%]
Ethanol production	25.4	1	0	0	0	0
	[6.0%]	[12.5%]	[0%]	[0%]	[0%]	[0%]
Fertilizer production	0	0	7,883.6	3	453.2	3
	[0%]	[0%]	[37.0%]	[15%]	[6.2%]	[17.6%]
Industrial	282.2	8	1,570.1	20	215.1	2
	[3.2%]	[7.1%]	[2.6%]	[6.0%]	[0.2%]	[0.4%]
Petroleum/natural gas processing	5,046.0	20	10,109.0	103	92.4	2
	[13.3%]	[6.4%]	[19.5%]	[15.4%]	[0.6%]	[0.7%]
Refineries/ chemicals	0	0	70,214.8	53	28.8	1
	[0%]	[0%]	[33.1%]	[19.1%]	[0.1%]	[0.6%]

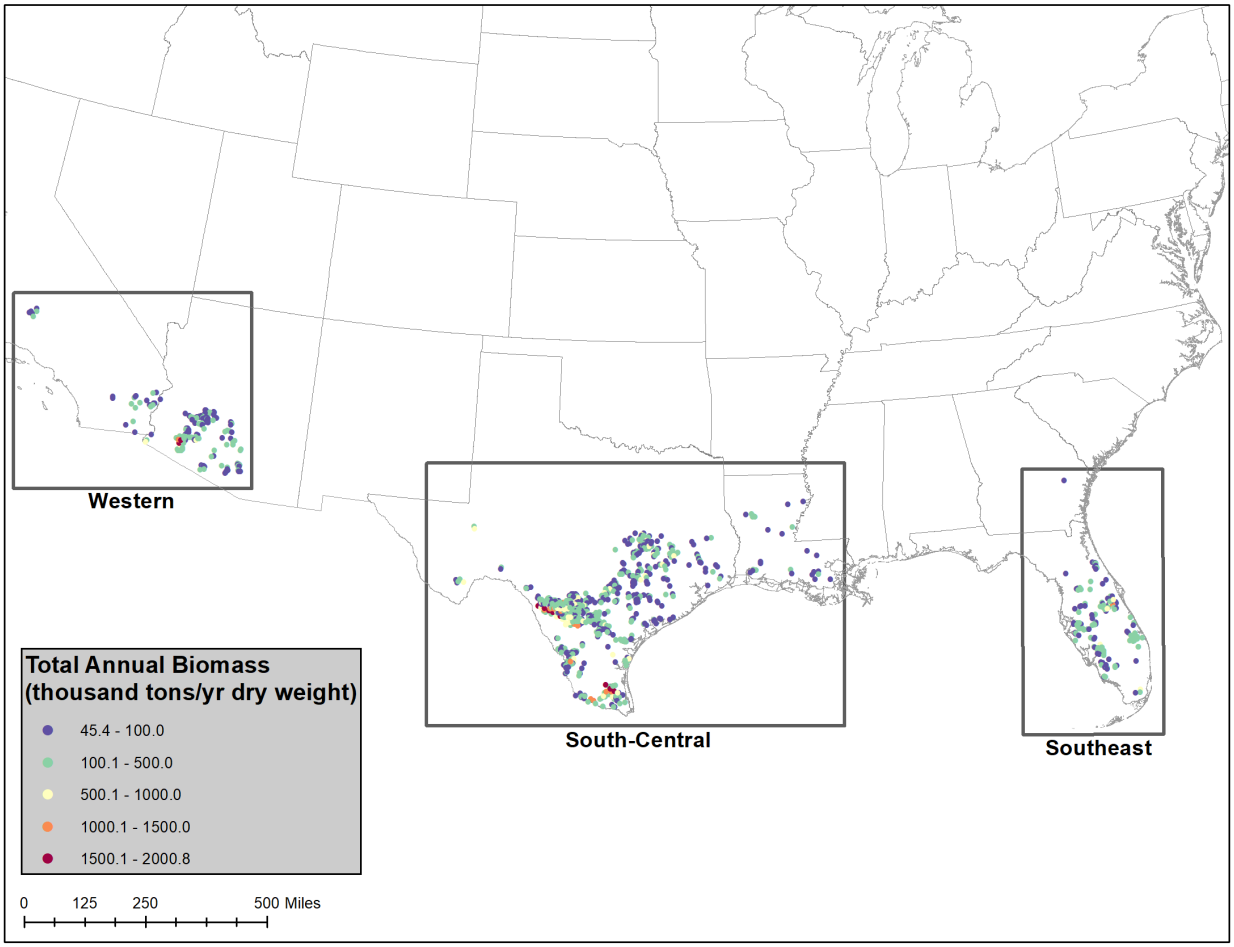

Figure 7.9. Total annual algae biomass (thousand tons/year dry weight) as modeled across identified farm sites

As documented in further detail in the 2022 microalgae model harmonization report (Davis et al. 2024), selected outputs from the BAT models were run through the algae farm TEA models, namely site-specific details for long-term monthly cultivation productivities, captured and delivered CO_2 costs, pond evaporation rates and associated saline groundwater well drilling and pumping power per volume of makeup saline water delivered at each site, forward osmosis system costs and associated power demands per volume of blowdown water processed, and brine injection disposal well development and respective pumping costs per volume of water injected (with water balances calculated in the farm models to achieve 55,000 mg/L or less salt content at harvest, followed by 15,000 mg/L or less salt content following the wash step through final dewatering for downstream delivery to conversion). The TEA models were run for each individual location, and the results presented here reflect individual location modeling granularity.

Figure 7.10 provides a summary of locations screened from the BAT models organized by regional group, overlaid with resultant MBSPs from the algae farm TEA models prior to seasonal storage. The resultant 152 million tons/yr of total algal biomass production potential

(AFDW basis) equates to 191 million tons/yr dry weight at 20% biomass ash content, as attributed to the BETO future target cultivation productivity of 25 g/m^2/day. Consistent with prior findings (Davis et al. 2016, 2018), the overall MBSP trends track closely with cultivation productivities (higher productivities translate to lower MBSPs), though with additional factors also weighing on MBSP results, particularly individual farm scale (larger farms incur economy-of-scale advantages), delivered CO_2 costs, water access, blowdown processing and disposal costs, and the degree of seasonal variability swings between peak versus minimum productivity (higher variability translates to greater seasonal storage needs/costs, as well as more total biomass subject to storage degradation losses). Table 7.2 presents a summary of key parameters organized by region, with biomass cost breakouts shown in the appendix for selected individual farms.

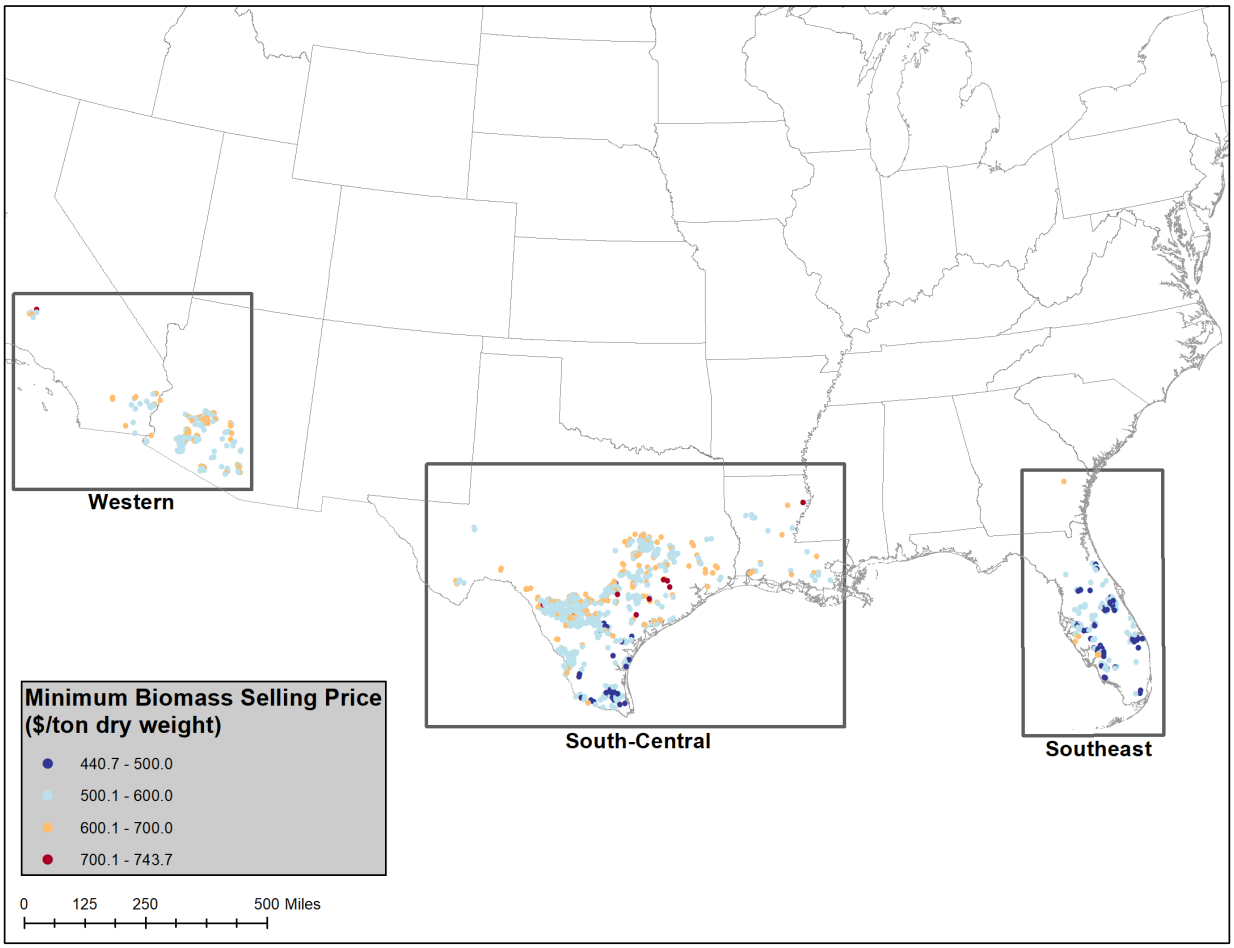

Figure 7.10. Pre-storage MBSP ($/ton dry weight) as organized by regional group

Table 7.2. Key Metrics for Algae Farm Availability and Cultivation Productivity for the Regional Groupings

Region	Number of Individual Sites	Total Cultivation Area (acres)	Total Biomass Output (million tons/year AFDW)	Annual Productivity (g/m²/day AFDW)	Annual Yield (tons/acre-year dry weight)	Productivity Variability (max vs. min ratio)
Western	168	521,395	19.7	24.9	47.5	6.2
South-Central	675	2,903,983	112.6	25.8	48.7	5.7
Southeast	137	434,091	19.6	29.8	56.6	3.0
Total/avg.	980	3,859,469	151.9	26.2	49.5	5.4

Figure 7.11 presents curves for MBSP versus cumulative algal biomass production, both on an AFDW basis (light green curve), as is more standard in algae TEA, and a dry weight basis (gray curve), as is more comparable to other biomass feedstock types presented in this report, based on individual farm TEA modeling prior to seasonal storage. Additionally, a translation to $/MMBtu biomass energy content versus cumulative dry weight production is provided (dark green curve), recognizing the higher costs for microalgal biomass compared to other terrestrial feedstocks presented in this report, but also the higher inherent energy content, and thus fuel yield potential, than many other feedstocks. The energy content curve is based on an HHV of 20.0 MJ/kg dry weight typical for microalgae across a number of strains (Illman, Scragg, and Shales 2000; Ghayal and Pandya 2013; Shakya et al. 2017; Coimbra, Escapa, and Otero 2019). After first excluding sites in the resource assessment stage that exceed thresholds of $75/tonne delivered CO_2 and 40,000 mg/L makeup water salinity, a small number of additional sites were removed following the algae farm TEA modeling stage after applying a maximum cutoff of $1,000/ton MBSP (AFDW basis). Still, the cost curve is seen to increase more sharply beginning at roughly $800/ton AFDW, primarily reflecting sites with smaller farm scales, lower cultivation productivity, and/or higher makeup water salinity (incurring higher blowdown handling costs).

These results present an overall average pre-storage MBSP of $674/ton AFDW ($536/ton dry weight) commensurate with the cumulative production potential of 152 million tons/yr of AFDW biomass (191 million tons/yr dry weight), equating to a price of $31.2/MMBtu biomass energy content (HHV) on average. After subsequently including seasonal storage to equalize the flows sent to downstream conversion processing (outside the scope of this chapter), MBSPs increase by roughly 4% on average (average MBSP = $701/ton AFDW after seasonal storage). The results presented here translate to 268 million tons/year of CO_2 uptake potential to produce this quantity of biomass.

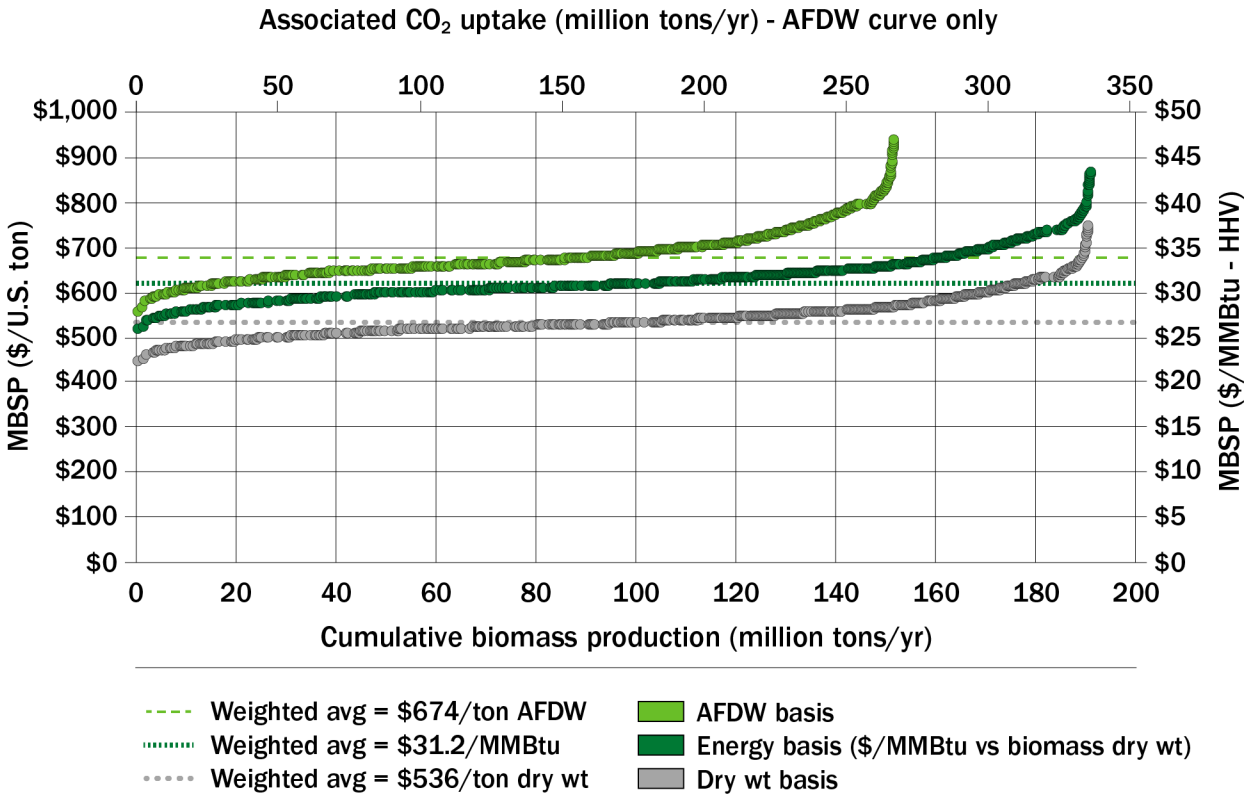

Figure 7.11. Biomass cost versus resource curves for MBSP in dollars per ton AFDW (light green curve), dollars per ton dry weight (gray curve), and dollars per MMBtu HHV energy content (dark green curve; dry weight biomass basis). Top axis for CO_2 uptake potential corresponds to the AFDW curve only.

7.1.4 Summary and Future Research

This update leverages the latest resource and techno-economic analyses for microalgal biomass as documented in the *2022 Algae Harmonization Update* study. As summarized here, that work highlights the potential to produce up to 152 million tons/yr of AFDW algal biomass across the CONUS, equating to 191 million tons/yr dry weight at roughly 20% ash content for high-salinity algal cultivation, attributed to 3.9 million acres of total available cultivation area with access to available saline groundwater water and point-source waste CO_2. This translates to an average biomass yield of 39.4 tons/acre-yr AFDW (49.5 tons/acre-yr dry weight). This material could be produced at an MBSP ranging from roughly $554 to $934 per ton AFDW, with an overall average for the identified farm sites of $674/ton AFDW (corresponding to $536/ton dry weight basis at a price of $31.2/MMBtu total HHV energy content). In turn, this resource volume reflects the ability to uptake 268 million tons/yr (9.6% of national CO_2 total) of waste flue gas captured CO_2 for subsequent upgrading to fuels and products. For context, the amount of CO_2 that can be fixed into microalgae each year is equivalent to the CO_2 output of the nation's 16 largest electricity generating stations.

Future research in this space includes opportunities to expand into lower-cost waste algae resources such as municipal wastewater treatment and collection of harmful algal blooms, as

these may represent opportunities for substantially lower-cost algal biomass (albeit at more limited quantities) and thus more readily deployable systems in the near term. Additionally, longer-term opportunities exist to consider direct air capture as a means to supplement or eventually replace dependency on non-biogenic point-source CO_2 availability, as this availability may decrease over time with continued industry decarbonization. Direct air capture could further unlock higher total algal biomass given CO_2 availability, and economically viable capture and transport from the point source to the algal farm, is a key limiting factor in the current study's resource analysis screening criteria. Alternatively, if the billion-ton study's projections are realized for other terrestrial biomass feedstock availability as discussed in this report (subsequently destined for biorefinery conversion and resultant biogenic CO_2 release), more biogenic CO_2 point sources may become available for utilization in algae farming as could further supplement this resource. This presents an opportunity for future consideration.

References

Bioenergy Technologies Office (BETO). 2020. *Bioenergy Technologies Office R&D State of Technology 2020*. Washington, D.C.: BETO. DOE/EE-2531. bioenergykdf.net/sites/default/files/2022-05/BETO-2020-SOT_FINAL_5-11-22.pdf.

Bleakley, S., and M. Hayes. 2017. "Algal proteins: extraction, application, and challenges concerning production." *Foods* 6 (5): 33.

Brennan, L., and P. Owende. 2010. "Biofuels from microalgae – A review of technologies for production, processing, and extractions of biofuels and co-products." *Renewable and Sustainable Energy Reviews* 14 (2): 557–577.

Cai, J., A. Lovatelli, J. Aguilar-Manjarrez, L. Cornish, L. Dabbadie, A. Desrochers, S. Diffey, et al. 2021. *Seaweeds and microalgae: an overview for unlocking their potential in global aquaculture development*. Rome, Italy: FAO Fisheries and Aquaculture Circular No. 1229. doi.org/10.4060/cb5670en.

Caporgno, M.P., and A. Mathys. 2018. "Trends in Microalgae Incorporation into Innovative Food Products with Potential Health Benefits." *Front. Nutr.* 5 (58).

Clippinger, J., and R. Davis. 2021. *Techno-Economic Assessment for Opportunities to Integrate Algae Farming with Wastewater Treatment.* Golden, CO: National Renewable Energy Laboratory. NREL/TP-5100-75237.

Coimbra, R.N., C. Escapa, and M. Otero. 2019. "Comparative thermogravimetric assessment on the combustion of coal, microalgae biomass and their blend." *Energies* 12 (15). doi: 10.3390/en12152962.

Coleman, A.M., J.M. Abodeely, R.L. Skaggs, W.A. Moeglein, D.T. Newby, E.R. Venteris, and M.S. Wigmosta. 2014. "An integrated assessment of location-dependent scaling for microalgae biofuel production facilities" *Algal Research* 5: 79–94. doi: 10.1016/j.algal.2014.05.008.

Davis, R., C. Kinchin, J. Markham, E.C.D. Tan, L.M.L. Laurens, et al. 2014. *Process Design and Economics for the Conversion of Algal Biomass to Biofuels: Algal Biomass Fractionation*

to Lipid-and Carbohydrate-Derived Fuel Products. Golden, CO: National Renewable Energy Laboratory.

Davis R., J. Markham, C. Kinchin, N. Grundl, E. Tan, and D. Humbird. 2016. *Process Design and Economics for the Production of Algal Biomass: Algal Biomass Production in Open Pond Systems and Processing Through Dewatering for Downstream Conversion*. Golden, CO: National Renewable Energy Laboratory.

Davis, R., J.N. Markham, C.M. Kinchin, C. Canter, J. Han, Q. Li, et al. 2018. *2017 Algae Harmonization Study: Evaluating the Potential for Future Algal Biofuel Costs, Sustainability, and Resource Assessment from Harmonized Modeling*. Golden, CO: National Renewable Energy Laboratory. NREL/TP-5100-70715. doi.org/10.2172/1468333.

Davis, R., T. R. Hawkins, A. Coleman, S. Gao, B. Klein, M. Wiatrowski, Y. Zhu, et al. 2024. *Economic, Greenhouse Gas, and Resource Assessment for Fuel and Protein Production from Microalgae: 2022 Algae Harmonization Update*. Golden, CO: National Renewable Energy Laboratory. NREL/TP-5100-87099. www.nrel.gov/docs/fy24osti/87099.pdf.

Devi, M.A., G. Subbulakshmi, K.M. Devi, and L.V. Venkataraman. 1981. "Studies on the proteins of mass-cultivated, blue-green alga (Spirulina platensis)." *Journal of Agricultural and Food Chemistry* 29 (3): 522–525.

———. 2021. "Global seaweeds and microalgae production, 1950-2019." Fact sheet. fao.org/3/cb4579en/cb4579en.pdf.

García, J. L., M. De Vicente, and B. Galán. 2017. "Microalgae, old sustainable food and fashion nutraceuticals." *Microbial Biotechnology* 10 (5): 1017.

Ghayal, M.S., and M.T. Pandya. 2013. "Microalgae biomass: A renewable source of energy." *Energy Procedia* 32: 242–250.

Huesemann, M. H., J. Van Wagenen, T. Miller, A. Chavis, S. Hobbs, and B. Crowe. 2013. "A screening model to predict microalgae biomass growth in photobioreactors and raceway ponds." *Biotechnology and Bioengineering* 110: 1583–1594. doi:10.1002/bit.24814.

Huesemann, M., S. Edmundson, S. Gao, S. Negi, T. Dale, A. Gutknecht, H. E. Daligault, et al. 2023. "DISCOVR strain pipeline screening–Part I: Maximum specific growth rate as a function of temperature and salinity for 38 candidate microalgae for biofuels production." *Algal Research* 71: 102996.

Huntley, M. E., Z. I. Johnson, S. L. Brown, D. L. Sills, L. Gerber, I. Archibald, S. C. Machesky, J. Granados, C. Beal, and C. H. Greene. 2015. "Demonstrated large-scale production of marine microalgae for fuels and feed." *Algal Research* 10: 249–265.

Illman, A.M., A.H. Scragg, and S.W. Shales. 2000. "Increase in Chlorella strains calorific values when grown in low nitrogen medium." *Enzyme and Microbial Technology* 27 (8): 631–635.

Jones, S., Y. Zhu, D. Anderson, R. Hallen, D. Elliott, A. Schmidt, et al. 2014. *Process Design and Economics for the Conversion of Algal Biomass to Hydrocarbons: Whole Algae Hydrothermal Liquefaction and Upgrading*. PNNL-23227.

Judd, S., L.J.P. van den Broeke, M. Shurair, Y. Kuti, and H. Znad. 2015. "Algal remediation of CO_2 and nutrient discharges: A review." *Water Research* 87: 356–366.

Klein, B., and R. Davis. 2022. *Algal Biomass Production via Open Pond Algae Farm Cultivation: 2021 State of Technology and Future Research*. Golden, CO: National Renewable Energy Laboratory. NREL/TP-5100-82417.

Langholtz, M. H., B. J. Stokes, and L. M. Eaton. 2016. *2016 Billion-Ton Report: Advancing Domestic Resources for a Thriving Bioeconomy*. Washington, D.C.: DOE. DOE/EE-1440.

Laurens, L.M.L., J. Markham, D.W. Templeton, E.D. Christensen, S. Van Wychen, E.W. Vadelius, M. Chen-Glasser, et al. 2017. "Development of algae biorefinery concepts for biofuels and bioproducts; a perspective on process-compatible products and their impacts on cost-reduction." *Energy & Environmental Science* 10: 1716–1738.

Miara, A., P.T. Pienkos, M. Bazilian, R. Davis, and J. Macknick. 2014. "Planning for algal systems: An energy-water-food nexus perspective." *Industrial Biotechnology* 10 (3). doi:10.1089/ind.2014.0004.

Molino, A., A. Iovine, P. Casella, S. Mehariya, S. Chianese, A. Cerbone, J. Rimauro, and D. Musmarra. 2018. "Microalgae characterization for consolidated and new application in human food, animal feed and nutraceuticals." *International Journal of Environmental Research and Public Health,* 15 (11): 2436.

Ou, L., S. Banerjee, H. Xu, A.M. Coleman, H. Cai, U. Lee, M.S Wigmosta, and T.R. Hawkins. 2021. "Utilizing high-purity carbon dioxide sources for algae cultivation and biofuel production in the United States: Opportunities and challenges." *J. Clean. Prod.* 321: 128779.

Reed, V., Z. Haq, A. Wiselogal, I. Rowe, M. Shmorhun, and S. Dillard. 2023. "DOE's Progress Toward Meeting the Goals of the SAF Grand Challenge." U.S. Department of Energy webinar, Feb. 22, 2023. energy.gov/sites/default/files/2023-03/beto-022223-saf-webinar-presentation_0.pdf.

Shakya, R., S. Adhikari, R. Mahadevan, S.R. Shanmugam, H. Nam, E.B. Hassan, and T. Dempster. 2017. "Influence of biochemical composition during hydrothermal liquefaction of algae on product yields and fuel properties." *Bioresource Technology* 243: 1112–1120.

Song, C., Q. Liu, N. Ji, S. Deng, J. Zhao, Y. Li, Y. Song, and H. Li. 2018. "Alternative pathways for efficient CO_2 capture by hybrid processes—A review." *Renewable and Sustainable Energy Reviews* 82: 215–231.

Sun, N., R. Skaggs, M.S. Wigmosta, A. Coleman, M.H. Huesemann, and S.J. Edmundson. 2020. "Growth Modeling to Evaluate Alternative Cultivation Strategies to Enhance National Microalgal Biomass Production." *Algal Research* 49: 101939. doi:10.1016/j.algal.2020.101939.

Venteris, E.R., R. McBride, A.M. Coleman, R. Skaggs, and M.S. Wigmosta. 2014. "Siting algae cultivation facilities for biofuel production in the United States: trade-offs between growth rate, site constructability, water availability, and infrastructure." *Environmental Science & Technology* 48 (6): 3559–3566. doi:10.1021/es4045488.

Wiatrowski, M., B. Klein, C. Kinchin, Z. Huang, and R. Davis. 2022. *Opportunities for Utilization of Low-Cost Algae Resources: Techno-Economic Analysis Screening for Near-Term Deployment*. Golden, CO: National Renewable Energy Laboratory. NREL/TP-5100-81780.

Wigmosta, M.S., A.M. Coleman, E.R. Venteris, and R.L. Skaggs. 2017. "Microalgae Feedstocks for Aviation Fuels." In *Green Aviation: Aircraft Technology, Alternative Fuels and Public Policy*. E.S. Nelson and D.R. Reddy (Eds.). Sustainable Energy Developments Series. New York: CRC Press, Taylor & Francis Group.

Xu, H., U. Lee, A.M. Coleman, M.S. Wigmosta, N. Sun, T. Hawkins, and M. Wang. 2020. "Balancing water sustainability and productivity objectives in microalgae cultivation: siting open ponds by considering seasonal water-stress impact using AWARE-US." *Environmental Science & Technology* 54 (4): 2091–2102. doi:10.1021/acs.est.9b05347.

Zhu, Y., S.B. Jones, A.J. Schmidt, J.M. Billing, D.M. Santosa, and D.B. Anderson. 2020. "Economic impacts of feeding microalgae/wood blends to hydrothermal liquefaction and upgrading systems." *Algal Research* 51: 102053.

7.2 Macroalgae

Andre Coleman,[1] Kristen Davis,[2] Julianne DeAngelo,[2] Troy Saltiel,[1] Benjamin Saenz,[3] Lee Miller,[1] Kathleen Champion,[4] Eliza Harrison,[5] and Anne Otwell[6]

[1] Pacific Northwest National Laboratory, Earth Systems Predictability & Resiliency Group
[2] University of California, Irvine, Department of Civil & Environmental Engineering
[3] Biota.Earth
[4] U.S. Department of Energy, Advanced Research Projects Agency–Energy (ARPA-E)
[5] Ocean Rainforest
[6] U.S. Department of Energy Bioenergy Technologies Office

Suggested citation: Coleman, A., K. Davis, J. DeAngelo, T. Saltiel, B. Saenz, L. Miller, K. Champion, E. Harrison, and A. Otwell. 2024. "Chapter 7.2: Macroalgae." In *2023 Billion-Ton Report*. M. H. Langholtz (Lead). Oak Ridge, TN: Oak Ridge National Laboratory. doi: 10.23720/BT2023/2316176.

Summary

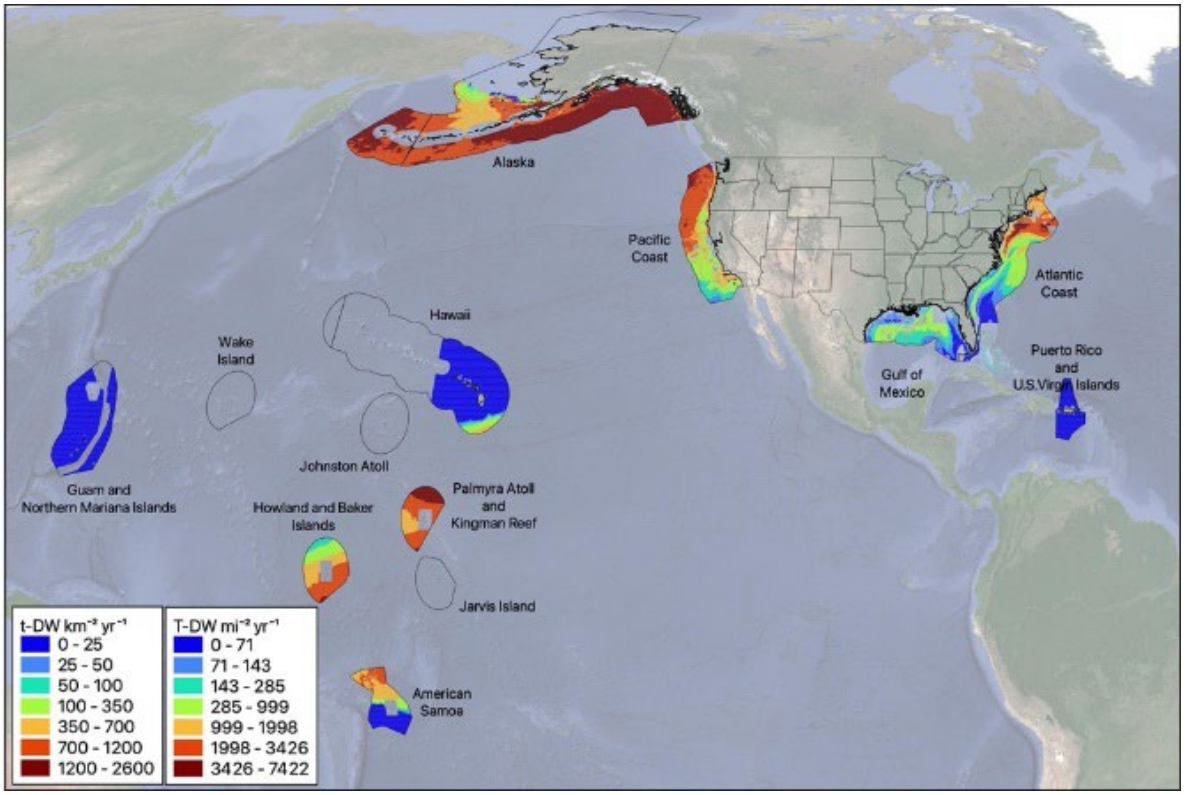

Figure 7.12. U.S. exclusive economic zone (EEZ) with screened-inclusive areas showing annual macroalgae biomass productivity estimates for the representative scenario

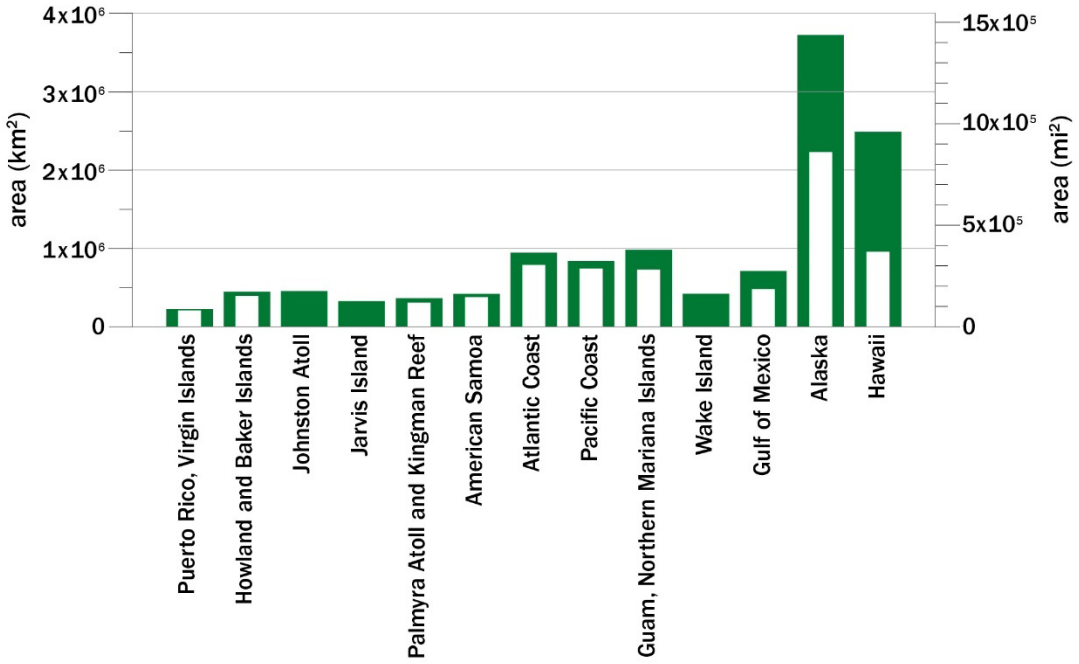

Figure 7.13. Total EEZ area by region (green bars) and remaining screened-inclusive areas (white bars) across the 13 specific regions

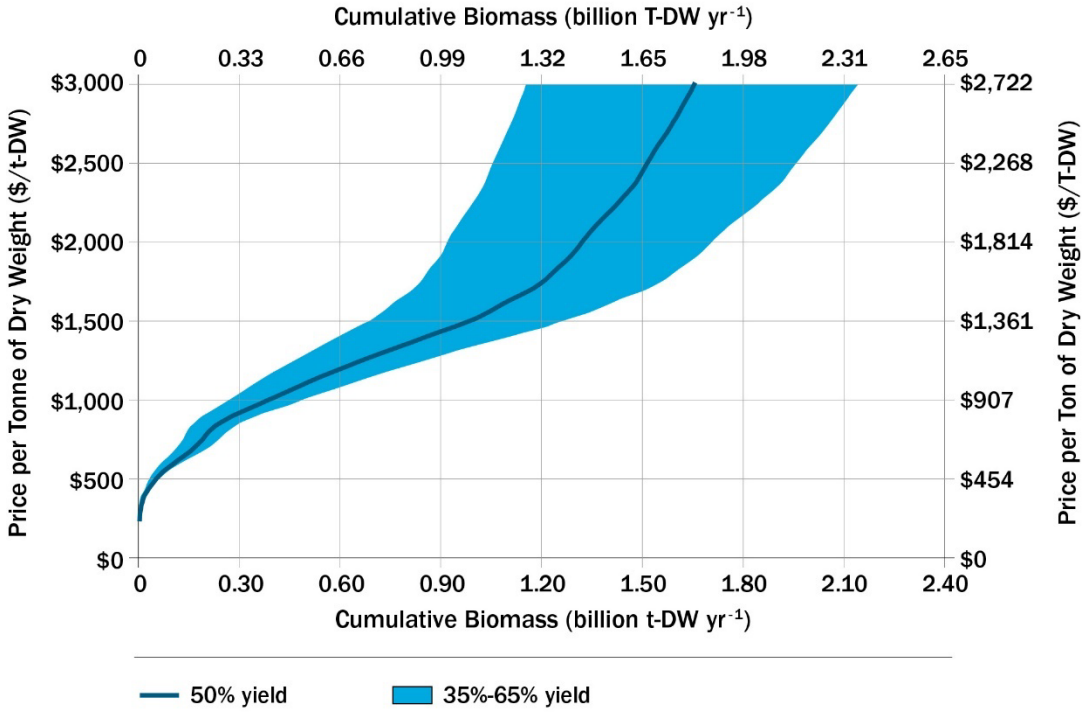

Figure 7.14. Cost-supply curve of the total U.S. EEZ for the representative scenario at 35%, 50%, and 65% area coverage

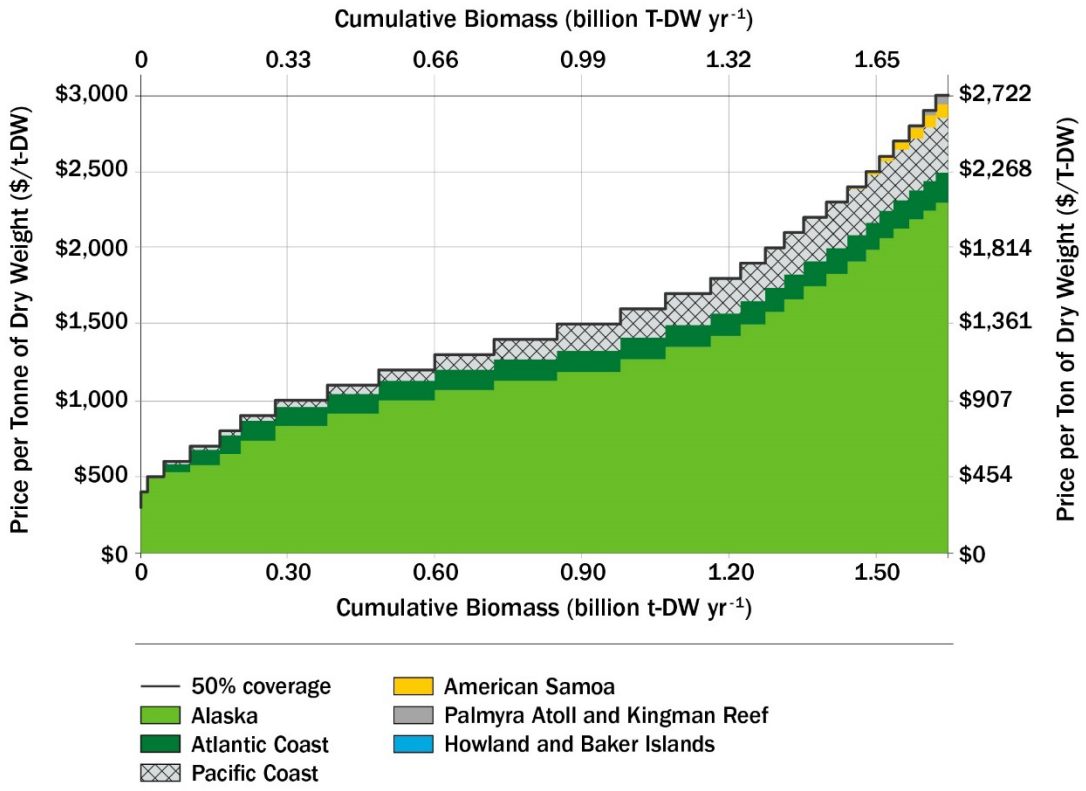

Figure 7.15. Region-specific stepwise cost-supply curve with the representative scenario and 50% area coverage. Note that unlisted regions have costs exceeding $3,000/t-DW.

This study represents the first U.S. full exclusive economic zone (EEZ) analysis for macroalgae biomass potential, inclusive of a marine area screening analysis, macroalgae biomass growth model, and associated TEA with harvest and farm gate biomass delivery.

- Of the total U.S. EEZ, 58.5% (7.1 million km^2, or 2.8 million mi^2) is potentially available for macroalgae cultivation after accounting for existing conflicting uses of marine spatial areas through a multi-criteria screening process.
- The unrestricted high-end annual biomass production over the screened marine areas estimated by the model is 3.3 billon metric tons of dry weight per year (Gt-DW/yr), or 3.6 billion short tons of dry weight per year (BT-DW/yr), which is about 34 times the mass of corn used for U.S. ethanol production and about 8 times the total U.S. corn production in 2022.[4] While this tonnage is approximately 3 times the total of the mature-market medium scenario for non-algal terrestrial sources estimated in this report, the actualizable tonnage is heavily restricted by non-mature technology and high costs.
- Utilizing a cost threshold of ≤$1,000 per metric ton of dry weight (t-DW) and a multi-criteria marine spatial area screening, a total of 293,000 km^2 in the Alaska, Pacific, and Atlantic coastal regions were identified as having the capacity to generate approximately

[4] Section 7.2 uses the following unit abbreviations: t (metric ton), T (U.S. short ton, or 200 lb.), BT (billion short tons), Gt (billion metric tons, or gigatons), and DW (dry weight).

0.38 Gt of macroalgae biomass per year (0.42 BT-DW/yr), with an estimated average farm gate cost of $739/t-DW ($670/T-DW).

7.2.1 Introduction

Macroalgae, commonly known as "seaweed," are diverse and abundant marine algae that play an important role in marine ecosystems. They not only are vital sources of food and habitat for a wide range of marine organisms, but also have significant ecological, economic, and cultural value (Neori et al. 2004). Macroalgae have been used by humans for centuries for food, medicine, and industrial applications. In the food industry, macroalgae are directly consumed; used as a source of vitamins, minerals, and dietary fiber; and used as a natural food colorant and flavor enhancer. For example, brown macroalgae, such as kelp, can contain high levels of dietary fiber, minerals (e.g., calcium, iodine, iron), and vitamins (e.g., vitamins C and K) (Holdt and Kraan 2011). The use of macroalgae (e.g., *Asparagopsis taxiformis*) as a supplement in animal feed is being investigated as a strategy for reducing methane emissions from cows and improving the nutritional quality of milk (Hristov et al. 2015; Vijn et al. 2020; Wasson et al. 2022).

Macroalgae are also used to produce a wide range of chemical products. For example, the polysaccharide alginate, which is derived from brown macroalgae, is widely used in the food, pharmaceutical, and textile industries as a thickener, stabilizer, and emulsifier (Rehm and Moradali 2018). Carrageenan, another polysaccharide derived from red macroalgae, is used as a gelling and thickening agent in food products such as ice cream, yogurt, and processed meats (Garcia-Vaquero et al. 2017). Fucoidan, a sulfated polysaccharide found in brown macroalgae, has been shown to have anti-inflammatory, anti-cancer, and antiviral properties, and is being developed as a nutraceutical and pharmaceutical ingredient (Fitton and Stringer 2019).

Macroalgae have also been identified as a potentially sustainable source of biomass and bioenergy due to their high growth rates, low lignin content, and high lipid and carbohydrate content (Godvin-Sharmila et al. 2021). An additional advantage is that macroalgae can be cultivated in marine environments, making them a potential source of renewable energy without competition for land and water resources. Studies have shown that macroalgae can be converted into bioenergy (biobutanol, bioethanol, biodiesel, biohydrogen, and biomethane) through various methods, including fermentation, hydrothermal liquefaction, anaerobic digestion, transesterification, and pyrolysis (Pourkarimi et al. 2019).

Macroalgae also have the potential to play a role in carbon sequestration and/or utilization (Krause-Jensen and Duarte 2016). As photosynthetic organisms, macroalgae absorb inorganic carbon from the surrounding water during growth. They utilize this source of carbon, along with sunlight and nutrients, to perform photosynthesis and produce biomass. It is important to note that the exact potential of macroalgae to sequester carbon depends heavily on factors such as species, carbon-to-nitrogen ratio, growth rates, cultivation methods, fate of the biomass (e.g., percent of biomass buried permanently in sediments or transformed into forms of carbon that are not easily bioavailable), ecosystem conditions, biogeochemical feedbacks (e.g., nutrient reallocation), and atmosphere-ocean CO_2 exchange (Bach et al. 2021; Hurd et al. 2022). Ongoing

research in this area aims to deepen our understanding of carbon flow within both natural and cultivated seaweed systems. The objective is to assess the extent of CO_2 removal and establish reliable methods for attributing carbon sequestration to seaweeds.

Macroalgae cultivation has been practiced for centuries in countries such as China, Japan, and Korea, where it is a traditional food and a major industry (FAO 2018). However, macroalgae cultivation is a relatively new industry in the United States, with most commercial production occurring in Maine and Alaska (Kim, Stekoll, and Yarish 2019). Despite this, the global macroalgae industry has grown significantly in recent years, with the total area of farms increasing by 42% between 2011 and 2016 (FAO 2018). China is the largest producer of macroalgae, accounting for more than 60% of global production, followed by Indonesia and the Republic of Korea. In comparison, the United States accounts for less than 0.1% of global macroalgae production (FAO 2018). The low level of macroalgae cultivation in the United States is attributed to a lack of infrastructure, technical expertise, and market development. However, there is increasing interest in the potential of macroalgae cultivation in the United States, where it could provide numerous economic and environmental benefits including the creation of new jobs, the production of renewable energy, and the reduction of GHG emissions (Kim, Stekoll, and Yarish 2019).

This study is the first comprehensive analysis of macroalgae biomass potential across the full EEZ of the United States. The analysis includes (1) a dynamic macroalgae growth model (Arzeno-Soltero et al. 2023) that competes four commonly cultivated seaweed groups (red and brown temperate and red and brown tropical seaweeds) with two bounding nutrient scenarios; (2) a TEA that incorporates industry-standard farm designs, harvest practices, and farm gate biomass delivery (DeAngelo et al. 2023); and (3) a marine spatial uses dataset derived through a newly developed multi-criteria marine area screening model.

7.2.2 Methods Summary

Biophysical Model

Farmed macroalgae yields are estimated by the Global MacroAlgae Cultivation MODeling System (G-MACMODS), a dynamical biophysical model incorporating constraints from extrinsic (environmental forcing) and intrinsic factors (biological parameters such as growth rates, nitrate uptake, nitrogen exudation, and mortality, among others) (Arzeno-Soltero et al. 2023). G-MACMODS uses macroalgae biomass and nitrogen as model currencies, and globally simulates four macroalgae types, each with distinct parameterizations of temperature tolerance, nitrogen uptake, light adaptation, and crowding capacity (a form of density dependence): tropical red, tropical brown, temperate red, and temperate brown. These parameterizations combine dynamically with input environmental parameters, macroalgae health (nitrogen status), and crowding to define the macroalgae growth rate. The macroalgae type with the highest yield in each grid cell was competed and selected for further analysis. The G-MACMODS model grid resolution is 1/12º (approximately 9 km or 5.6 mi at the equator) and uses a daily time step for growth and harvest calculations.

The model uses inputs of surface nitrate concentration (Long and Saenz 2023), sea surface temperature, surface chlorophyll-*a* concentration, downward shortwave irradiance (Behrenfeld and Falkowski 1997; Ocean Productivity 2022), current speed (Global Ocean Forecasting System 2022), and significant wave height and period (European Centre for Medium-Range Weather Forecasts 2022). To gauge potential yield, seeding/out-planting timing and harvest were optimized across 17 years (2003–2019) of model inputs; non-optimized harvest schedules are also available (based on current farming practices). A limited-nutrient scenario is also available, where nitrate available for macroalgae growth is limited to an estimate of natural renewal from vertical ocean transport processes (upwelling and mixing), and which is more representative of restricted nutrient availability under intensive seaweed cultivation practices. G-MACMODS simulations analyzed here assume no artificial macronutrient amendments and do not include riverine nitrate (runoff). Final yield calculations were made using inputs from 2017, the most recent year with available data that is identified with having a neutral El Niño–Southern Oscillation index.

Macroalgae Techno-Economic Model

The macroalgae techno-economic model is based on the methodology detailed in DeAngelo et al. (2023) and modified to represent the cost of end-use-agnostic macroalgae biomass delivered to shore. The cost of harvested macroalgae biomass is estimated using all costs related to the macroalgae farming process, up to and including the point of harvest at the farm location, as well as costs related to the transportation of harvested biomass to the nearest port. Calculations were made using metric units, and the final results are also reported in imperial units. A high-level representation of the techno-economic model is presented in Figure 7.16.

Spatially explicit costs of macroalgae production are calculated based on annual macroalgae biomass productivity (t-DW/km^2) of the highest-yielding macroalgae type in each grid cell, cultivation line spacing, and harvest interval (species-dependent) from the G-MACMODS biophysical growth model, as well as ranges of capital costs (\$/km^2), operating costs (including labor, \$/km^2), harvest costs (\$/km^2), and transport costs (\$/t/km) from the ARPA-E Macroalgae Research Inspiring Novel Energy Resources (MARINER) farm partners and the scientific literature (Table 7.3; appendix; ARPA-E 2023). The "distance to the nearest port (km)" (Global Fishing Watch 2020) is used to calculate the cost of transporting the harvested macroalgae biomass (wet weight) to the "farm gate," defined here as delivery to shore. This is analogous to terrestrial energy crop availability after harvest and delivery to roadside. Datasets of ocean depth (m) (General Bathymetric Chart of the Oceans 2022) and significant wave height (m) (European Centre for Medium-Range Weather Forecasts 2022) are used to estimate spatially explicit increases in capital costs due to increased anchoring depth and the impact of rough seas on equipment lifetime, respectively.

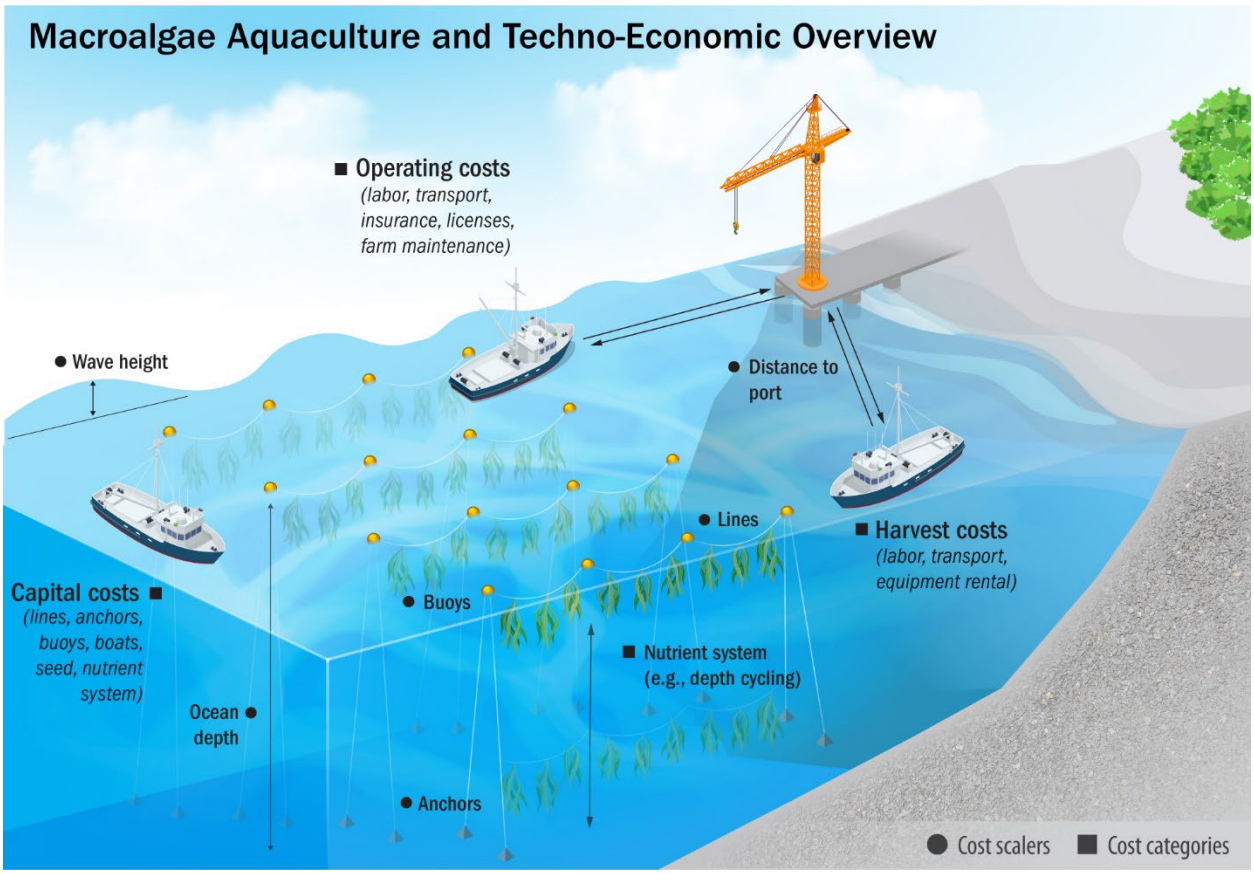

Figure 7.16. High-level overview of the major components influencing macroalgae productivity and capital and operational expenses, all of which comprise the techno-economic model

To assess uncertainty in our estimates that arise from both widely varying farm cost data and uncertainty in the G-MACMODS biomass output, three techno-economic scenarios are assessed: (1) a low-yield, low-cost scenario; (2) a medium-yield, low-cost scenario; and (3) a high-yield, high-cost scenario (Table 7.3). The medium-yield, low-cost scenario is highlighted throughout this chapter as the representative scenario for cost results and is reflective of a scenario where the biomass yield is based on ambient nutrients, but harvesting and seeding schedules are based on current practices. See Section 7.2.2: Methods Summary for more information. Scenario 2 is contrasted with Scenario 3, where potential future technology allows for highly optimized harvest and seeding timing, which would likely require substantial cost increases. Results from the "low-yield, low-cost" and "high-yield, high-cost" scenarios, as well as a detailed scenario of cost inputs, are detailed in the appendices.

Table 7.3. The Framework for Three Techno-Economic Macroalgae Cultivation Scenarios

	Scenario 1 (Low Yield, Low Cost)	Scenario 2 (Representative Scenario) (Medium Yield, Low Cost)	Scenario 3 (High Yield, High Cost)
Biophysical Model			
Nutrient case	Limited nutrients	Ambient nutrients	Ambient nutrients
Seeding and harvesting condition	Standard practices (non-optimized)	Standard practices (non-optimized)	Optimized practices
Techno-Economic Model			
Summary	Costs reflect limited nutrient yield using standard practices (low input costs and no nutrient replenishment system)	Costs reflect ambient nutrient yield using standard practices (low input costs, but nutrient replenishment system required)	Costs reflect fully optimized ambient nutrient yield (high input costs for optimization and nutrient system required)
Cost framework	Minimum of MARINER costs (scaled to model farm footprint)	Minimum of MARINER costs (scaled to model farm footprint) plus nutrient system cost	75th percentile of MARINER costs (scaled to model farm footprint) plus nutrient system cost

Further techno-economic modeling assumptions are provided in the following appendices:

- Production Cost Calculation Overview
- Capital Cost Inputs and Calculations
- Operating and Maintenance Cost Inputs and Calculations
- Harvest Cost Inputs and Calculations
- Transport Cost Inputs and Calculations
- Cost Model Parameter Input Values
- Low-Yield, Low-Cost Scenario Results
- High-Yield, High-Cost Scenario Results.

Marine Spatial Planning

Marine spatial planning is a relatively new process, mostly developed over the last two decades, and focuses on balancing ecological, economic, and social needs (Ehler 2021). Initial efforts were at the state level, with Oregon adopting the Oregon Territorial Sea Plan in 1994, followed by Massachusetts, Rhode Island, and New York—partially driven by offshore wind farm

proposals (Portman et al. 2009; Ehler 2021). Federally, the National Oceanic and Atmospheric Administration (NOAA) National Centers for Coastal Ocean Science (NCCOS) provide ecological and socioeconomic data and scientific support for coastal and offshore managers (NCCOS 2023). NOAA and the Bureau of Ocean Energy Management maintain MarineCadastre.gov (marinecadastre.gov/), a source for authoritative ocean data and tools, and NCCOS provides coastal planning and siting products and services to support aquaculture. The marine environment is dynamic, with potentially harsh and varying physical conditions and complex laws and regulations (Roesijadi et al. 2011; Silverman-Roati, Webb, and Gerrard 2021).

Unlike other analyses in this report that are limited to the CONUS, this analysis is based on a resource that is only available outside the CONUS and thus includes a different spatial extent. Specifically, to assess the macroalgae productivity and techno-economic potential, the entire U.S. EEZ was used, inclusive of the coastal waters around the CONUS, Alaska, Hawaii, and the 14 U.S. territories (Figure 7.17). The surface area of the U.S. EEZ is vast, encompassing 24% more surface area (12.2 million km^2, or 4.7 million mi^2) than the total U.S. onshore area (9.9 million km^2, or 3.8 million mi^2). To date, NOAA has performed the most intensive analysis of marine areas for aquaculture opportunity, though for limited regions. For example, the Southern California Bight (Morris et al. 2021) and Gulf of Mexico (Riley et al. 2021) NOAA Aquaculture Opportunity Area atlases document 395 stakeholder engagement sessions that were held with a total of 1,848 participants (NOAA 2021).

This analysis utilizes the methods developed in NOAA's Aquaculture Opportunity Analysis atlases to identify the most conflicting areas. These conflicting areas are defined as uses or features that NOAA considers as constraints, or areas excluded for aquaculture purposes. The associated geospatial data encompass the broader categories of natural and cultural resources, national security, industry, navigation, transportation, and fishing and aquaculture, with most data sourced from NOAA (Figure 7.18; appendix). Any area that intersects the conflicting areas was masked out (screened) before considering the results from the biophysical and techno-economic models. The screening analysis is performed at a 200-m grid resolution, and features like submarine cables, ferry routes, wrecks, and obstructions had a minimum linear width of 1 km (Figure 7.19). This high-resolution screening layer was resampled to 1/12° spatial resolution to match the G-MACMODS biophysical and techno-economic models by taking the majority (screened/not screened) within each model grid cell. The resampling process reduced some of the detail of the screening, no longer capturing areas with a few cables or ferry lines (relatively small areas) but retaining larger features like unexploded ordinance areas. The result is that any grid cell that is not screened contains mostly nonconflicting use, and the uncertainty in the exact value can be reflected with farm area coverage scenarios. This screened-inclusive model layer was then used to calculate representative yield and cost.

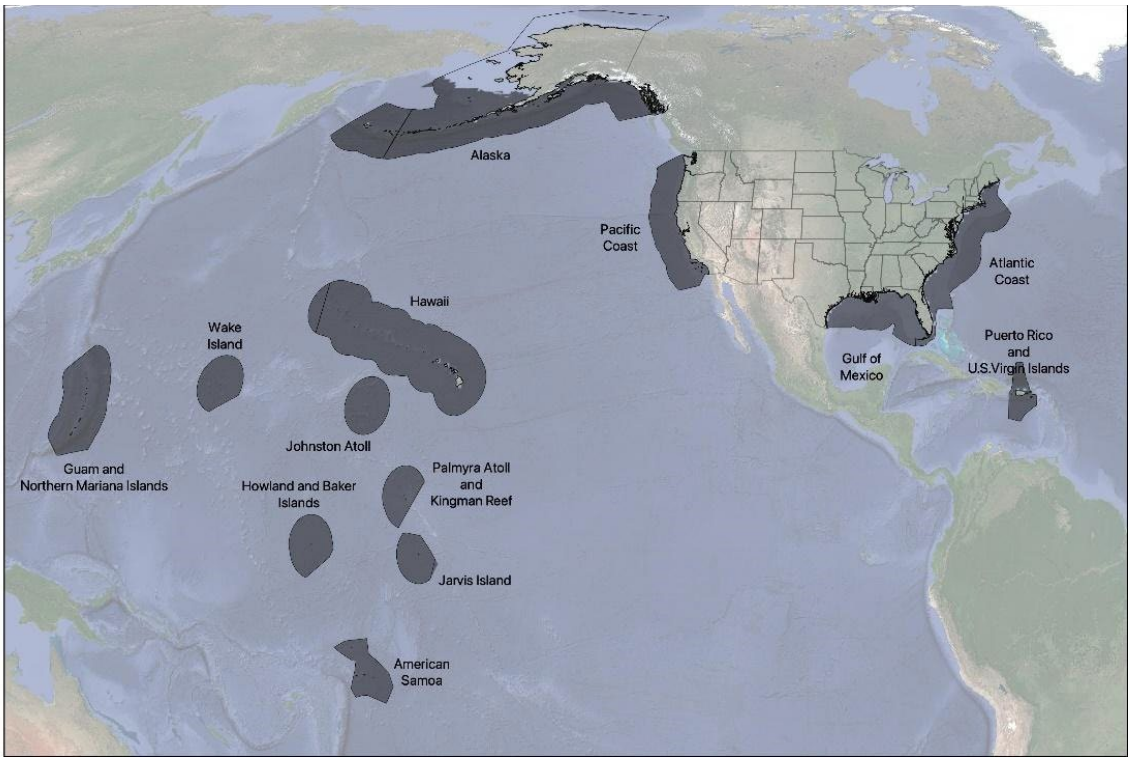

Figure 7.17. The U.S. EEZ considered in this analysis (gray polygons) has an area of 12.2 million km^2 (4.7 million mi^2).

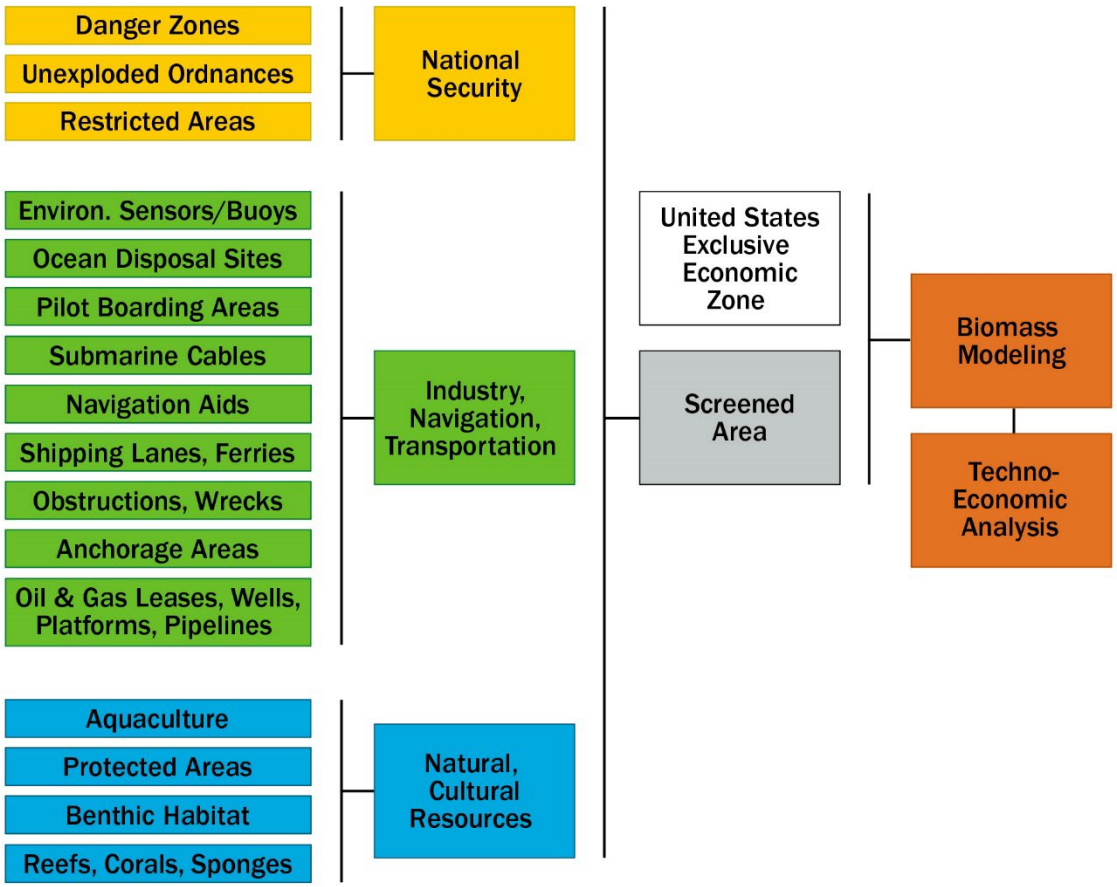

Figure 7.18. General marine area screening methodology based on NOAA's Aquaculture Opportunity Area workflow. Screened areas are merged with G-MACMODS biomass productivity and TEAs.

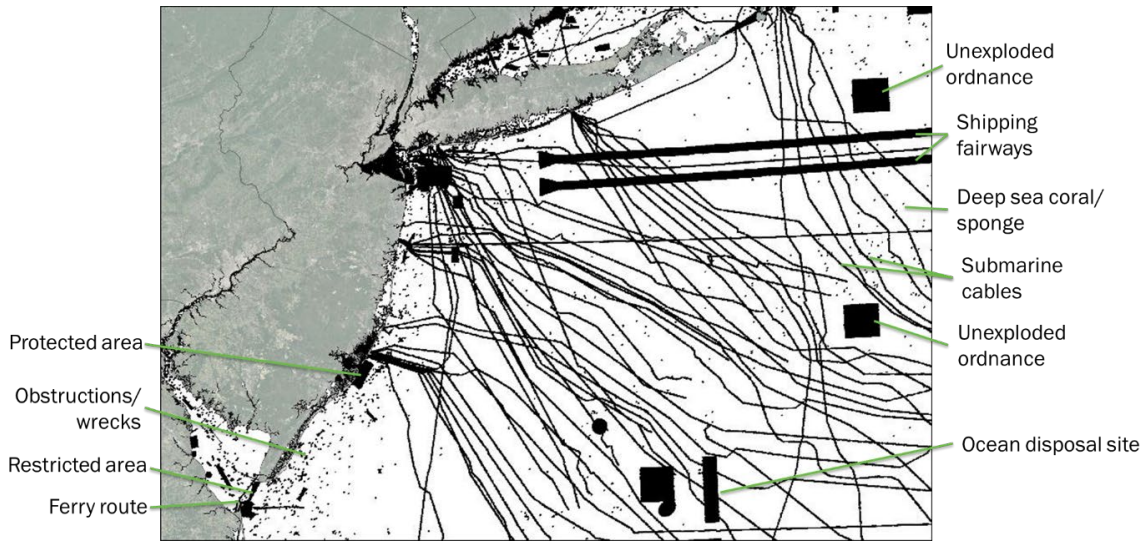

Figure 7.19. Example marine screening inclusion/exclusion analysis. The base spatial resolution of this analysis is 200 m. The black areas represent conflicting areas because of an existing use, and thus not appropriate for macroalgae cultivation.

Using the representative scenario, cost-supply curves were generated for each region to determine the possible yield at four cost thresholds: $500/t-DW, $1,000/t-DW, $2,000/t-DW, and $3,000/t-DW ($453/T-DW, $907/T-DW, $1,814/T-DW, and $2,722/T-DW, respectively). The cost thresholds are easily adapted to evaluate additional scenarios. The cost-supply curves utilize the lowest-cost areas first to generate the cumulative sum of annual biomass yield. As modeled, the yield estimates assume full utilization. In other words, outside of required line spacings within a given farm, all screened-inclusive areas are used. To better account for individual farm spacing, infrastructure/access channels within and between farms, coastline and outcrop features, conflicting use areas, and ecological sensitivities, three area yield utilization scenarios are considered: 65%, 50%, and 35% area coverage (see Figure 7.20 for general area coverage reference). The 50% area coverage provides a middle-ground scenario, while the 65% and 35% yield scenarios represent more and less optimistic estimates, respectively.

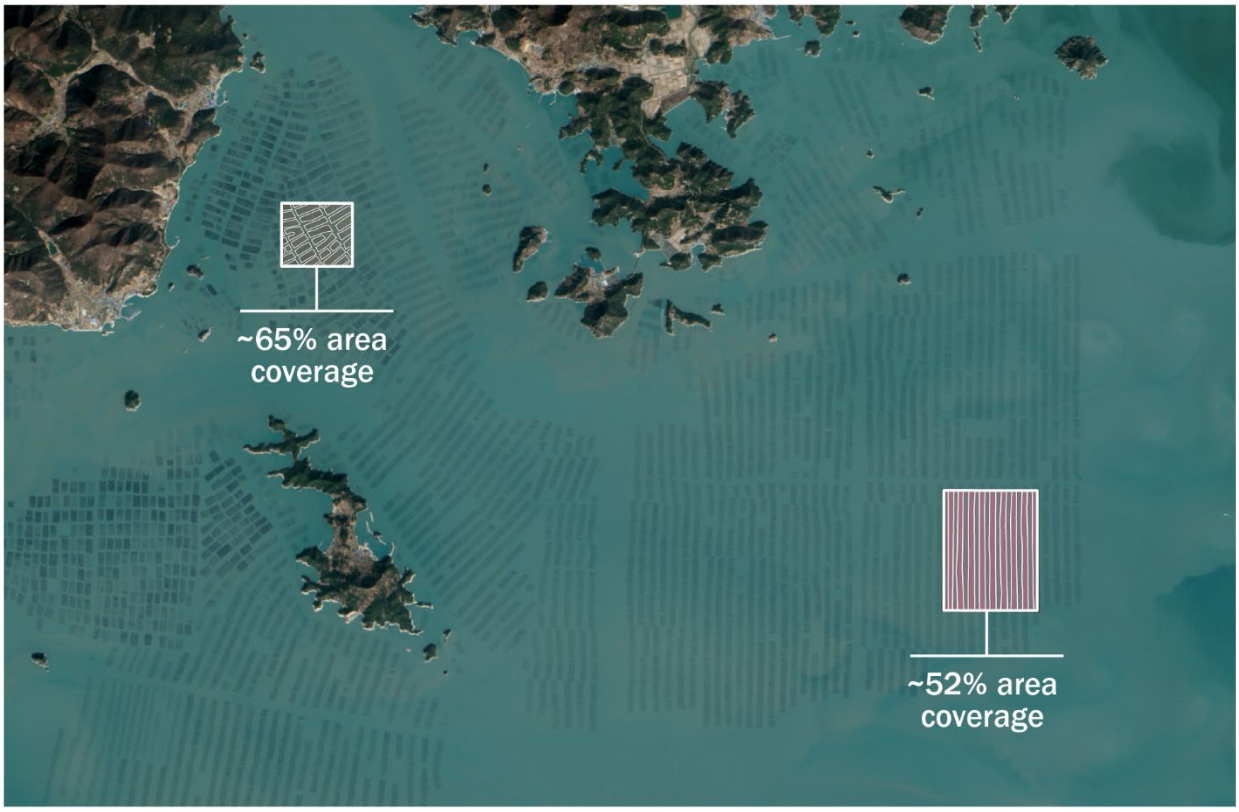

Figure 7.20. Examples of area coverage at existing macroalgae farm sites in the Republic of Korea.

Source: NASA 2015

7.2.3 Results

Screening for conflicting areas leaves 7.1 million km^2 (2.8 million mi^2) for possible macroalgae cultivation, which equates to 58.5% of the total 12.2 million km^2 (4.7 million mi^2) in the U.S. EEZ area. For reference, this equates to 72.3% of the U.S. onshore area (CONUS, Alaska, Hawaii, U.S. territories, and inland water bodies included). Different regions yield different levels of screening depending on environmental and safety protections, existing use, and other

defined constraints, with a summary shown in Figure 7.21. Detailed screened-inclusive area values are available in the appendix.

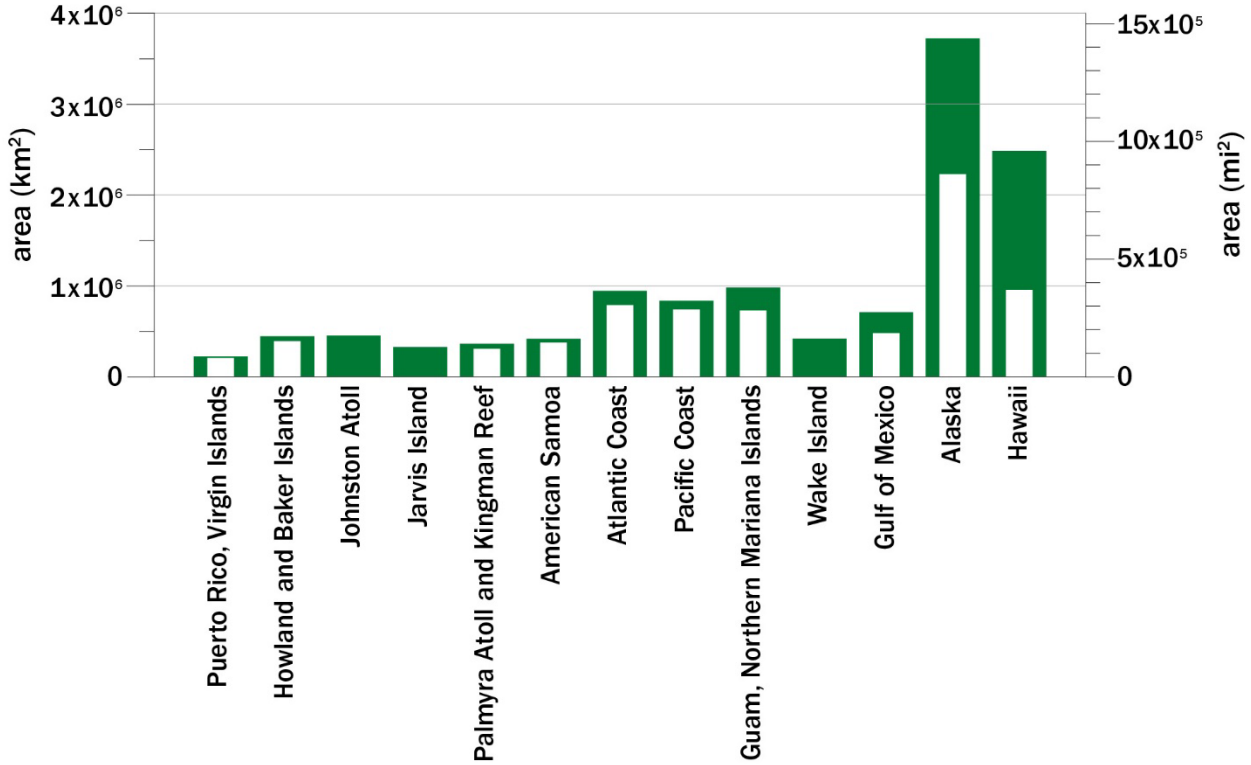

Figure 7.21. Total EEZ area by region (green bars) and remaining screened-inclusive areas (white bars) across the 13 specific regions

Areas of the highest macroalgae biomass productivity for the representative scenario are shown along the coastal and/or offshore areas of the northern Atlantic/New England; the U.S. West Coast (central to northern Pacific); southeastern Alaska and westward through the Aleutian Peninsula and islands; the South Pacific including Palmyra Atoll, Kingman Reef, Howland and Baker islands; and the northerly portion of American Samoa (Figure 7.22). At the U.S. EEZ scale, it is evident that expansive areas were excluded, and this is largely due to existing protected areas (e.g., western Hawaiian island chain, Wake Island, Johnston Atoll, and Jarvis Island). Generally, the areas showing lower macroalgae biomass productivity (e.g., Puerto Rico, U.S. Virgin Islands, Hawaii, Guam) are associated with low concentration of nutrients in the surface ocean. Areas with lower costs tend to be closer to shore and have higher biomass productivity and/or require fewer harvests for the same amount of biomass, since each additional harvest in the biophysical model has associated costs reflected in the techno-economic model (Figure 7.23). The model results for the Gulf of Mexico predict relatively low productivity due to low surface nutrient concentrations in model inputs. This result may be due to insufficient model resolution and freshwater input in this highly riverine-influenced region, and this is discussed as a limitation of the study in Section 7.2.5. The region-specific biomass productivity and techno-

economic mapping results provide more detail and are presented in the appendix, where pockets of higher productivity are shown (e.g., Southern California—San Diego and Catalina islands). Figure 7.24 shows the range of productivity and costs per region.

Evaluating the U.S. EEZ as a whole, considering the 65%, 50%, and 35% coverage areas within the screened-inclusive areas and cost thresholds of $500, $1,000, $2,000, and $3,000 per t-DW ($454, $907, $1,814, and $2,722 per T-DW), productivities range from 0.03 to 2.14 Gt-DW/yr (0.03 to 2.36 BT-DW/yr), and associated average costs range from $419 to $1,470 per t-DW ($380 to $1,333 per T-DW) (Table 7.4). To detail this further, a regional analysis by cost threshold is presented with $500/t-DW ($454/T-DW) (Table 7.5), $1,000/t-DW ($907/T-DW) (Table 7.6), $2,000/t-DW ($1,814/T-DW) (Table 7.7), and $3,000/t-DW ($2,722/T-DW) (Table 7.8). Note that there are 13 regions evaluated across the U.S. EEZ (Figure 7.17); if a specific region is not shown, it indicates it was excluded due to the aforementioned cost thresholds. The U.S. EEZ cost-supply curve for the representative scenario and different area coverage scenarios is presented in Figure 7.25. A region-specific stepwise cost-supply curve using the representative scenario and 50% area coverage is presented in Figure 7.26.

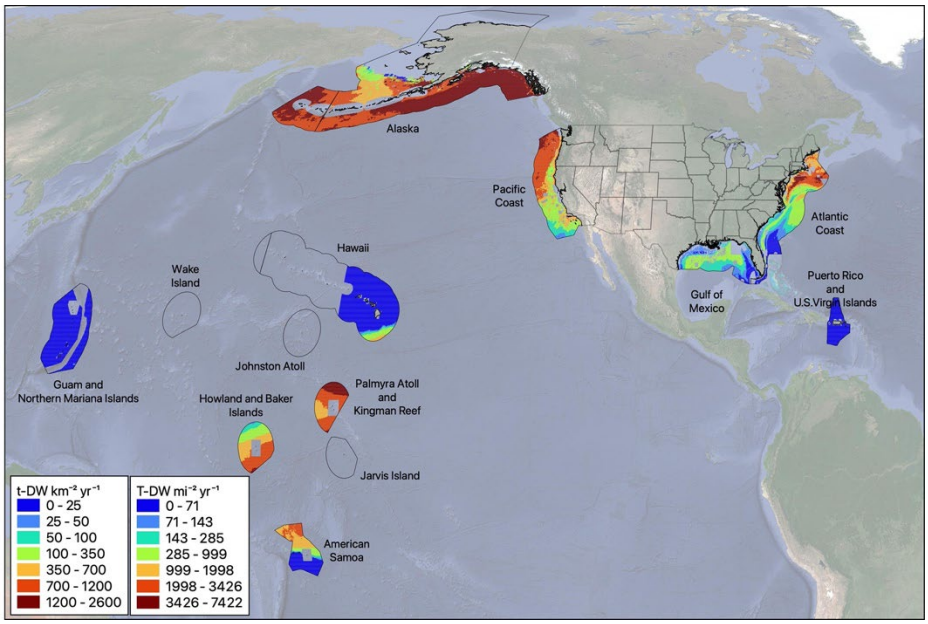

Figure 7.22. U.S. EEZ with screened-inclusive areas showing annual macroalgae biomass productivity estimates for the representative scenario

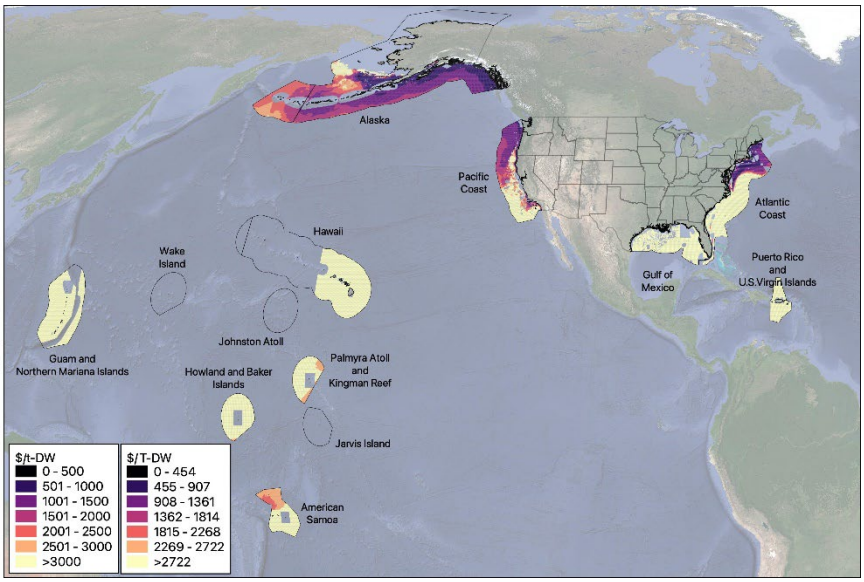

Figure 7.23. U.S. EEZ with screened-inclusive areas and techno-economic results for macroalgae biomass for the representative scenario, with areas >$3,000/t-DW (>$2,722/T-DW) being grouped into a common class

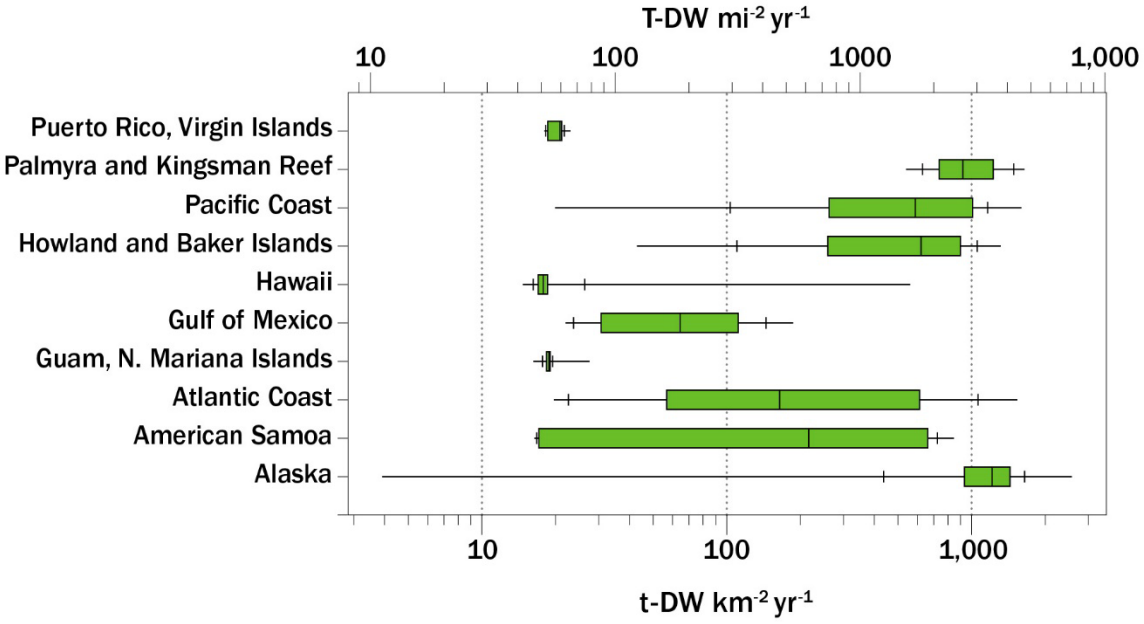

Figure 7.24. Full (100%) area productivity (top) and costs (bottom) of the representative scenario for each region. Each line extends from the minimum to the maximum value, with hashes shown at the 10th and 90th percentiles, boxes covering the 25th to 75th percentiles, and a 50th percentile line in the middle. Note that Wake Island, Johnston Atoll, and Jarvis Island are not included in the plots, as these areas were fully excluded during the marine area screening

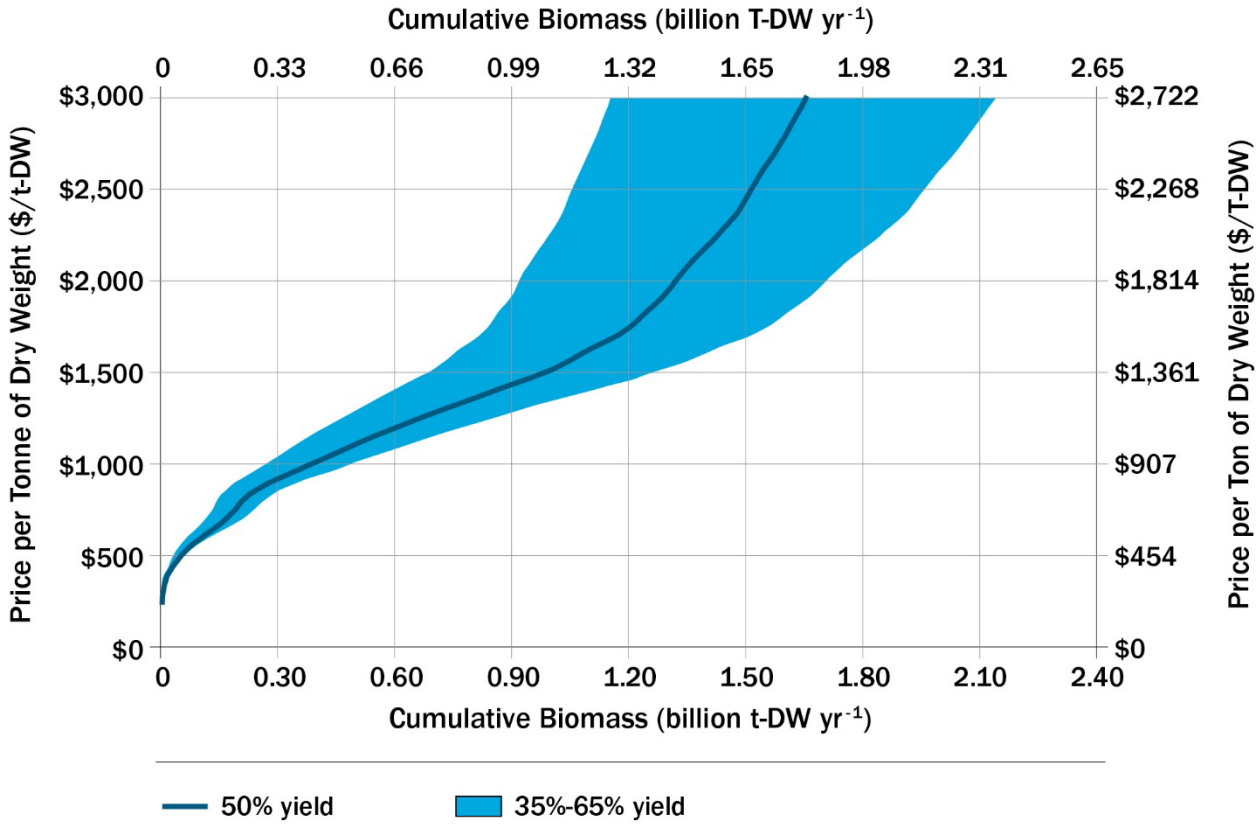

Figure 7.25. Cost-supply curve of the total U.S. EEZ for the representative scenario (Scenario 2) at 35%, 50%, and 65% area coverage

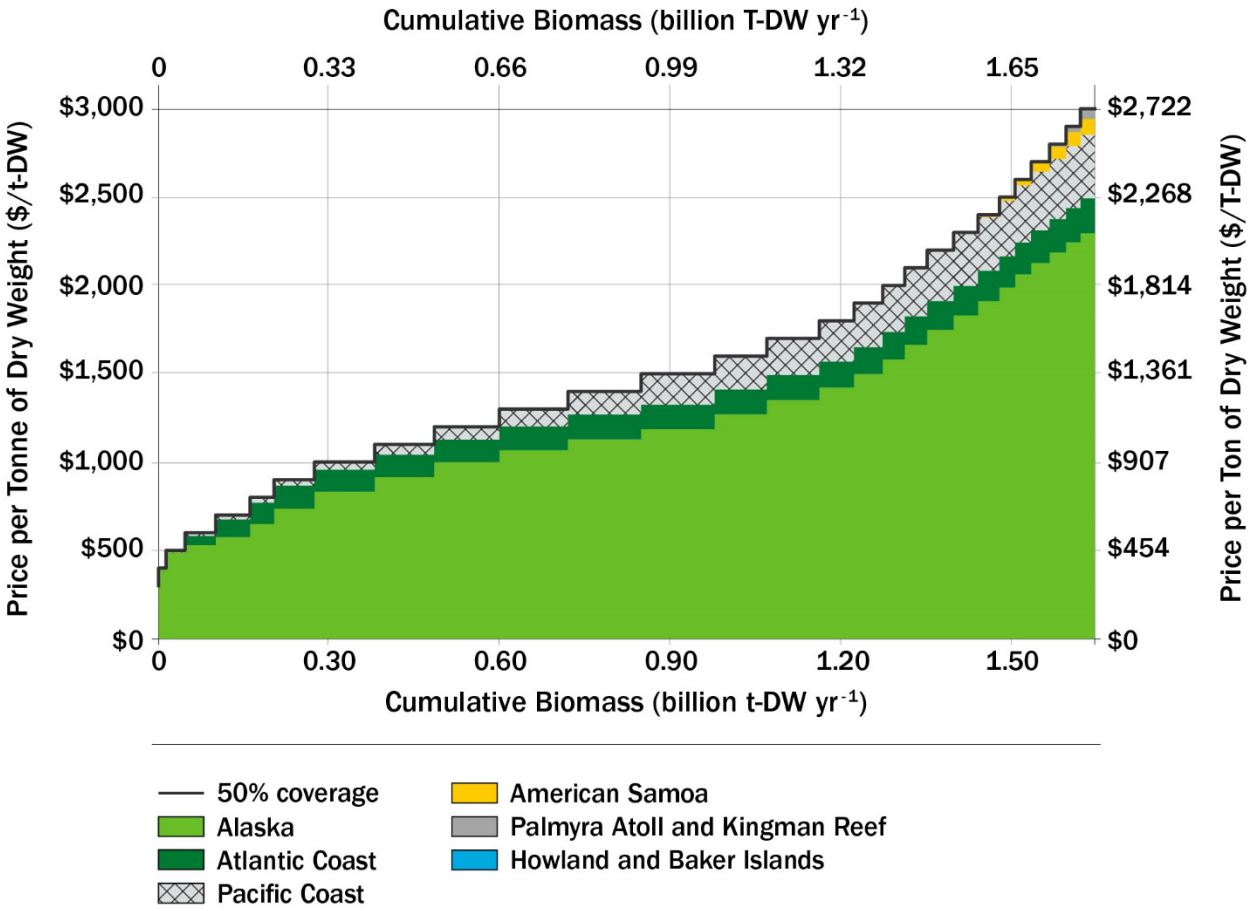

Figure 7.26. Region-specific stepwise cost-supply curve with the representative scenario and 50% area coverage. Note that unlisted regions have costs exceeding $3,000/t-DW.

Table 7.4. Summary of Total Annual U.S. EEZ Biomass Potential for the Representative Scenario at 65%, 50%, and 35% Coverage Areas and Cost Thresholds of $500, $1,000, $2,000, and $3,000 per t-DW ($454, $907, $1,814, and $2,722 per T-DW, Respectively)

Cost Cap ($/t-DW) [$/T-DW]	Area (km²) [mi²]	65% Coverage Area (Gt-DW/yr) [BT-DW/yr]	50% Coverage Area (Gt-DW/yr) [BT-DW/yr]	35% Coverage Area (Gt-DW/yr) [BT-DW/yr]	Average Cost ($/t-DW) [$/T-DW]
500 [454]	57,000 [22,008]	0.06 [0.07]	0.05 [0.05]	0.03 [0.04]	419 [380]
1,000 [907]	585,000 [225,869]	0.50 [0.55]	0.38 [0.42]	0.27 [0.29]	739 [670]
2,000 [1,814]	2,207,000 [852,124]	1.71 [1.88]	1.31 [1.45]	0.92 [1.01]	1,222 [1,108]
3,000 [2,722]	3,006,000 [1,160,618]	2.14 [2.36]	1.65 [1.82]	1.15 [1.27]	1,470 [1,333]

Table 7.5. Region-Specific Cost Threshold of $500/t-DW ($454/T-DW) at 65%, 50%, and 35% Coverage Area for the Representative Scenario

Region	Area (km²) [mi²]	65% Coverage Area (Gt-DW/yr) [BT-DW/yr]	50% Coverage Area (Gt-DW/yr) [BT-DW/yr]	35% Coverage Area (Gt-DW/yr) [BT-DW/yr]	Average Cost ($/t-DW) [$/T-DW]
Alaska	55,000 [21,236]	0.062 [0.068]	0.048 [0.052]	0.033 [0.037]	418 [380]
Pacific Coast	2,000 [772]	0.002 [0.002]	0.001 [0.001]	0.001 [0.001]	450 [408]

Table 7.6. Region-Specific Cost Threshold of $1,000/t-DW ($907/T-DW) at 65%, 50%, and 35% Coverage Area for the Representative Scenario

Region	Area (km²) [mi²]	65% Coverage Area (Gt-DW/yr) [BT-DW/yr]	50% Coverage Area (Gt-DW/yr) [BT-DW/yr]	35% Coverage Area (Gt-DW/yr) [BT-DW/yr]	Average Cost ($/t-DW) [$/T-DW]
Alaska	458,000 [176,834]	0.41 [0.46]	0.32 [0.35]	0.22 [0.24]	737 [669]
Atlantic Coast	93,000 [35,907]	0.06 [0.07]	0.05 [0.05]	0.03 [0.04]	733 [665]
Pacific Coast	34,000 [13,127]	0.02 [0.02]	0.02 [0.02]	0.01 [0.01]	788 [715]

Table 7.7. Region-Specific Cost Threshold of $2,000/t-DW ($1,814/T-DW) at 65%, 50%, and 35% Coverage Area for the Representative Scenario

Region	Area (km²) [mi²]	65% Coverage Area (Gt-DW/yr) [BT-DW/yr]	50% Coverage Area (Gt-DW/yr) [BT-DW/yr]	35% Coverage Area (Gt-DW/yr) [BT-DW/yr]	Average Cost ($/t-DW) [$/T-DW]
Alaska	1,621,000 [625,869]	1.35 [1.49]	1.04 [1.14]	0.73 [0.80]	1,208 [1,096]
Atlantic Coast	233,000 [89,961]	0.13 [0.15]	0.10 [0.11]	0.07 [0.08]	1,062 [964]
Pacific Coast	353,000 [136,293]	0.23 [0.25]	0.17 [0.19]	0.12 [0.13]	1,399 [1,269]

Table 7.8. Region-Specific Cost Threshold of $3,000/t-DW ($2,722/T-DW) at 65%, 50%, and 35% Coverage Area for the Representative Scenario

Region	Area (km²) [mi²]	65% Coverage Area (Gt-DW/yr) [BT-DW/yr]	50% Coverage Area (Gt-DW/yr) [BT-DW/yr]	35% Coverage Area (Gt-DW/yr) [BT-DW/yr]	Average Cost ($/t-DW) [$/T-DW]
Alaska	2,092,000 [807,722]	1.64 [1.81]	1.26 [1.39]	0.88 [0.97]	1,410 [1,279]
Atlantic Coast	258,000 [99,614]	0.14 [0.15]	0.11 [0.12]	0.08 [0.08]	1,132 [1,027]
Pacific Coast	461,000 [177,992]	0.26 [0.29]	0.20 [0.22]	0.14 [0.15]	1,527 [1,385]
American Samoa	142,000 [54,826]	0.06 [0.07]	0.05 [0.05]	0.03 [0.04]	2,626 [2,382]
Howland and Baker islands	4,000 [1,544]	0.003 [0.003]	0.002 [0.002]	0.002 [0.002]	2,943 [2,670]
Palmyra Atoll and Kingman Reef	49,000 [18,919]	0.04 [0.04]	0.03 [0.03]	0.02 [0.02]	2,859 [2,594]

7.2.4 Summary and Future Research

To our knowledge, this is the first U.S. EEZ-wide analysis for macroalgae biomass potential, inclusive of a marine area screening analysis, macroalgae biomass growth model, and associated TEA to the farm gate, defined as wet biomass delivery at the nearest port (Global Fishing Watch 2020). Using a cost cap of $1,000/t-DW ($907/T-DW) and 585,000 km^2 of marine area over portions of the Alaska, Atlantic, and Pacific coasts, 0.38 Gt-DW/yr (0.42 BT-DW/yr) could be produced assuming 50% of the marine area is productive, with an average cost of $739/t-DW ($670/T-DW). If the cost cap were lifted to $3,000/t-DW ($2,722/T-DW), production could expand across 3,006,000 km^2 of marine area. This would add portions of American Samoa, Howland and Baker islands, Palmyra Atoll, and Kingman Reef, producing 1.65 Gt-DW/yr (1.82 BT-DW/yr) under a 50% productive marine area, and at an average cost of $1,470 t-DW ($1,333/T-DW). High capital and operational costs of deep-water farm locations can make farming even in some high-yield regions cost prohibitive. For example, the EEZ water surrounding American Samoa and the Palmyra Atoll show high yields (Figure 7.22) due to the high nitrate conditions from equatorial upwelling in this region. However, the cost per tonne of seaweed yield is also very high (Figure 7.23), primarily due to high farming costs in deep waters. Transport cost is also a factor at the Palmyra Atoll (where no port exists), but still constitutes less than 10% of the total cost. It is, however, important to note that yields and costs presented here are reflective of the medium-yield, low-cost scenario, more representative of current, small-scale farm efforts. For high-intensity farming over large areas, the low-yield scenario is most relevant, as it considers nutrient competition between farms (see appendix).

Macroalgae as a biomass feedstock has significant potential, but production in the United States has yet to be realized, with relatively high costs associated with a new industry. This feedstock is unique compared to other biomass sources, as it would be situated over near-coastal and offshore waters, which, screening for conflicting uses, equates to 7.1 million km^2 of potential area. These conflicting uses include protected areas, military restrictions, and existing industry like oil and gas. While developing macroalgae resources remains a complex endeavor, aquaculture generally does not conflict with other biomass sources or land-based agriculture, meaning it is a complementary feedstock source that fits well within many of BETO's 2023 Multi-Year Program Plan objectives.

Given this massive area, the $1,000/t-DW ($907/T-DW) cost cap potential macroalgae production (under the 50% coverage area) of 0.38 Gt-DW (0.42 BT-DW) is about one-third of the total mature-market medium scenario for terrestrial feedstocks. The results reported here provide a representative medium-yield, low-cost scenario, where ambient nutrient sources are modeled and standard farm practices are implemented. While the costs may be considered optimistic, as they reflect minimum costs reported through the ARPA-E MARINER program for cutting-edge aquaculture technology (ARPA-E 2023), production costs will undoubtedly change with development and scaling of macroalgae farming in U.S. waters.

The biophysical modeling used in this work provides a dynamic model of potential macroalgae growth across four macroalgae types (tropical red, tropical brown, temperate red, and temperate brown) and does so on a large scale (U.S. EEZ) at reasonable spatial and temporal resolutions (1/12º, daily). The biophysical macroalgae biomass growth model includes environmental (e.g., downward shortwave irradiance, water temperature, ocean currents, wave heights, nutrient availability), biological (e.g., growth rate, crowding/shading) and farm configuration (e.g., line spacing, harvest time) factors, plus the selection of the best macroalgae type for an area. The techno-economic model represents the cost of macroalgae biomass cultivation and delivery to port, considering farm dynamics (line spacing and harvest interval), growth from the biophysical model, and capital costs (operating, harvest, and transport).

7.2.5 Present Assumptions, Limitations, and Future Work

G-MACMODS is a dynamic macroalgae growth model that estimates farm yield as constrained by environmental variables and farming practices. Several assumptions were made in the simulations reviewed above, which are described here briefly and in more detail in Arzeno-Soltero et al. (2023):

- G-MACMODS predictions assume that nitrogen is the limiting macronutrient for the growth of all seaweed groups and, further, that micronutrient supplementation (such as iron embedded within grow lines) will be deployed in areas deficient in trace minerals.
- The techno-economic model assumes that macroalgae is grown and harvested from an anchored floating array.

- Farming costs are modeled assuming longline (tropical brown, tropical red, temperate brown) or net (temperate red) arrays.
- The harvest and transport scheme assumes that macroalgae farming boats would travel the shortest sea-route distance between farms and the nearest port.

Modeled yields may vary (higher or lower) than actual yields due to model limitations:

- Biomass yields for locations near coastal rivers and/or sources of anthropogenic nutrient enhancement may be underestimated. Riverine and anthropogenic nitrate sources are not included in this version of the model.
- Wave erosion of macroalgae biomass is parameterized in G-MACMODS (Arzeno-Soltero et al. 2023), but the inherent variability in large storms and wave events for the many regions modeled results in uncertainty in this form of biomass loss.
- Pests, including grazers and epiphytes, as well as disease, are currently a large source of loss to macroalgae operations worldwide; episodic outbreaks are not simulated by G-MACMODS.

G-MACMODS is global-level model. Regional modeling products that can resolve local riverine nutrient inputs and mesoscale oceanographic features are recommended to guide exploration and investment in farm sites. The current marine area screening focuses on hard constraints, or areas where we are confident an existing use would conflict with macroalgae cultivation. However, there may be areas that were not screened that, in a more localized analysis, may still not be considered viable. Future marine spatial planning analysis could include social or cultural data (nearshore), species distributions, sensitive habitat, potential environmental impacts to the ecosystem, and impacts to shipping and navigation outside of designated shipping lanes (Farmer et al. 2022). The spatial analysis would also benefit from including collocation potential with existing infrastructure such as offshore wind or other future complementary marine energy projects, which could potentially reduce cost and minimize environmental and social impacts. A full suitability analysis, where a favorability score is produced, would help in selecting the best sites for macroalgae cultivation. Additional marine area screening limitations are documented in the appendix.

Separate from the technical considerations of the simulations, this analysis of yield and cost potential does not include the social, cultural, or environmental impacts from large-scale cultivation of macroalgae. Future macroalgae aquaculture marine spatial planning efforts and development projections will be improved by considering such impacts. Best efforts were made to include sustainability constraints in this analysis that account for limitations around environmental concerns. For example, exclusion areas and a reduction factor (35%, 50%, or 65%) were applied to account for constraints that are unknown, including ecological sensitivities. As a theoretical scoping analysis of an evolving resource, it is expected that more sustainability constraints could be added in the future, which could reduce potential supplies. Additionally, sensitivity and uncertainty analyses should be incorporated to reflect the dynamic nature of

meteorology, extreme events, and climate change, including projected changes in ocean conditions that can stress growing seaweeds such as rising sea surface temperature, increases in the frequency and severity of storms, and decreases in surface nitrate concentrations due to increases in stratification.

Lastly, the cases presented in this report do not incorporate a projected future learning curve. However, as the seaweed cultivation industry matures, it is expected that farmers will develop more efficient techniques and tools, leading to higher yields per cultivation area. This improved efficiency can result in reduced production costs as operational processes become optimized.

Case Study: Ocean Rainforest

Kate Champion and Eliza Harrison

Ocean Rainforest is among the leading pioneers of macroalgae-based aquaculture in the Western Hemisphere. In 2018, ARPA-E's MARINER program provided an opportunity for Ocean Rainforest and their partners to develop new technologies that would propel the macroalgae cultivation industry forward. The team proposed a pilot farm to demonstrate the feasibility of growing *Macrocystis* for commercial use. *Macrocystis* is native to the U.S. West Coast and is among the fastest-growing organisms on the planet.

Despite many obstacles, the team has successfully put lines in the water to begin cultivation. Now in their second year of production, they have managed yields of 25 kg wet weight per meter of line, well within range of model predictions. Over the course of the project, they have performed dozens of experiments to optimize yield, develop hatchery protocols with near 100% induction success, and refine their seeding methodology. Of note, aquaculture permitting in the United States is complex and split across local, state, and federal control, resulting in conflicting requirements that present time and resource challenges to aquaculture farmers.

Ocean Rainforest is moving forward under a limited permit to install the first deep-water offshore farm for macroalgae cultivation in the United States. This new site sits in 75–80 m of water approximately 5 miles from the Santa Barbara Harbor in the central California coastal area. Working in deep, open ocean waters (>50 m) is rare, even for major macroalgae-producing countries like South Korea. The deep-water site will also enable continued optimization of macroalgae cultivation strategies while continuing technical advancements and market development. Testing remote-operated vehicles with the capacity to install screw anchors could, for example, reduce farm footprint and associated mooring costs. Similarly, unmanned underwater vehicles equipped with cameras and sonar could drive down labor and monitoring costs associated with maintaining the farm. Data generated from the site will also help validate models that predict yield—helping to demonstrate the economic, social, and environmental benefits of macroalgae farming.

The planning is oriented toward the development of a 1,000-ha commercial site that would yield 10,000 t-DW/yr (11,023 T-DW/yr) based on modeling assessments. Such an operation would allow for a private industry operation to deliver a meaningful supply of regenerative biomass for the bioenergy, biofuel, and agricultural industries.

References

Advanced Research Projects Agency – Energy (ARPA-E). 2023. "Macroalgae Research Inspiring Novel Energy Resources (MARINER)." arpa-e.energy.gov/technologies/programs/mariner.

Arzeno-Soltero, I.B., C.A. Frieder, B.T. Saenz, M.C. Long, J. DeAngelo, S.J. Davis, and K.A. Davis. 2023. "Biophysical potential and uncertainties of global seaweed farming." *Communications Earth & Environment* (accepted).

Bach, L.T., V. Tamsitt, J. Gower, et al. 2021. "Testing the climate intervention potential of ocean afforestation using the Great Atlantic Sargassum Belt." *Nat Commun* 12: 2556. doi.org/10.1038/s41467-021-22837-2.

Behrenfeld, M. J., and P. G. Falkowski. 1997. "Photosynthetic rates derived from satellite-based chlorophyll concentration." *Limnology and Oceanography* 42 (1): 1–20.

DeAngelo, J., B. T. Saenz, I. B. Arzeno-Soltero, C. A. Frieder, M. C. Long, J. Hamman, et al. 2023. "Economic and biophysical limits to seaweed farming for climate change mitigation." *Nature Plants*, 9 (1): 45–57.

Ehler, C. N. 2021. "Two decades of progress in Marine Spatial Planning." *Marine Policy* 132: 104134.

European Centre for Medium-Range Weather Forecasts. 2022. "ECWMWF Reanalysis v5 (ERA5)." European Union Copernicus Climate Change Service. ecmwf.int/en/forecasts/dataset/ecmwf-reanalysis-v5.

Farmer, N. A., J. R. Powell, J. A. Morris Jr, M. S. Soldevilla, L. C. Wickliffe, J. A. Jossart, et al. 2022. "Modeling protected species distributions and habitats to inform siting and management of pioneering ocean industries: A case study for Gulf of Mexico aquaculture." *Plos One* 17 (9): e0267333.

Fitton, J. H., and D. N. Stringer. 2019. "Therapies from fucoidan: An update." *Marine Drugs* 17 (6): 327.

Food and Agriculture Organization of the United Nations (FAO). 2018. *The State of World Fisheries and Aquaculture 2018 (SOFIA) - Meeting the sustainable development goals*. Rome, Italy. fao.org/documents/card/en/c/I9540EN/.

García-Vaquero, M., G. Rajauria, J. V. O'Doherty, and T. Sweeney. 2017. "Polysaccharides from macroalgae: Recent advances, innovative technologies and challenges in extraction and purification." *Food Research International* 99: 1011–1020.

General Bathymetric Chart of the Oceans. 2022. "GEBCO_2022 Grid." gebco.net/data_and_products/historical_data_sets/#gebco_2022.

Global Fishing Watch. 2020. *Distance from port in meters*. Washington, D.C.: Global Fishing Watch. globalfishingwatch.org/data-download/datasets/public-distance-from-port-v1.

Global Ocean Forecasting System. 2022. "GOFS 3.1: 41-layer HYCOM + NCODA Global 1/12° Analysis." hycom.org/dataserver/gofs-3pt1/analysis.

Godvin-Sharmila, V., M. Dinesh-Kumar, A. Pugazhendi, A.K. Bajhaiya, P. Gugulothu, and R.B. J. 2021. "Biofuel production from Macroalgae: present scenario and future scope." *Bioengineered* 12 (2): 9216–9238.

Holdt, S. L., and S. Kraan. 2011. "Bioactive compounds in seaweed: functional food applications and legislation." *Journal of Applied Phycology* 23 (3): 543–597.

Hristov, A. N., J. Oh, F. Giallongo, T. W. Frederick, M. T. Harper, H. L. Weeks, et al. 2015. "An inhibitor persistently decreased enteric methane emission from dairy cows with no negative effect on milk production." *Proceedings of the National Academy of Sciences* 112 (34): 10663–10668.

Hurd, C.L., C.S. Law, L.T. Bach, D. Britton, M. Hovenden, E.R. Paine, J.A. Raven, V. Tamsitt, and P.W. Boyd. 2022. "Forensic carbon accounting: Assessing the role of seaweeds for carbon sequestration." *Journal of Phycology* 58 (3): 347–363.

Kim, J., M. Stekoll, and C. Yarish. 2019. "Opportunities, challenges and future directions of open-water seaweed aquaculture in the United States." *Phycologia* 58 (5): 446–461.

Krause-Jensen, D., and C. M. Duarte. 2016. "Substantial role of macroalgae in marine carbon sequestration." *Nature Geoscience* 9 (10): 737–742. doi.org/10.1038/ngeo2790.

Long, M., and B. Saenz. 2023. "Nitrate flux and inventory from high-resolution CESM CORE-Normal-Year integration." Version 1.0. UCAR/NCAR - GDEX. doi.org/10.5065/hpae-3j62.

Morris Jr., J. A., J. K. MacKay, J. A Jossart, L. C. Wickliffe, A. L. Randall, G. E. Bath, et al. 2021. *An Aquaculture Opportunity Area Atlas for the Southern California Bight*. NOAA Technical Memorandum NOS NCCOS 298, National Centers for Coastal Ocean Science.

NASA. 2015. "Seaweed Farms in South Korea." NASA Earth Observatory, EOS Project Science Office. earthobservatory.nasa.gov/images/85747/seaweed-farms-in-south-korea.

National Centers for Coastal Ocean Science (NCCOS). 2023. "Coastal and Marine Planning." coastalscience.noaa.gov/science-areas/coastal-and-marine-planning/.

National Oceanic and Atmospheric Administration (NOAA). 2021. *NOAA Fisheries Aquaculture Opportunity Area Updates*. National Marine Fisheries Service, NOAA. media.fisheries.noaa.gov/2021-12/Aquacuture-Atlases-AOA-Update-Slides.pdf.

Neori, A., T. Chopin, M. Troell, A. H. Buschmann, G. P. Kraemer, C. Halling, et al. 2004. "Integrated aquaculture: rationale, evolution and state of the art emphasizing seaweed biofiltration in modern mariculture." *Aquaculture* 231 (1–4): 361–391.

Ocean Productivity. 2022. "Ocean Productivity." Oregon State University. sites.science.oregonstate.edu/ocean.productivity/index.php.

Portman, M. E., J. A. Duff, J. Köppel, J. Reisert, and M. E. Higgins. 2009. "Offshore wind energy development in the exclusive economic zone: Legal and policy supports and impediments in Germany and the US." *Energy Policy* 37 (9): 3596–3607.

Pourkarimi, S., A. Hallajisani, A. Alizadehdakhel, and A. Nouralishahi. 2019. "Biofuel production through micro-and macroalgae pyrolysis–A review of pyrolysis methods and process parameters." *Journal of Analytical and Applied Pyrolysis* 142: 104599.

Rehm, B. H., and M. F. Moradali (Eds.). 2018. *Alginates and their biomedical applications*. Vol. 11: 1–268. Singapore: Springer.

Riley, K. L., L. C. Wickliffe, J. A. Jossart, J. K. MacKay, A. L. Randall, G. E. Bath, et al. 2021. *An Aquaculture Opportunity Area Atlas for the US Gulf of Mexico*. NOAA Technical Memorandum NOS NCCOS 299.

Roesijadi, G., A. M. Coleman, C. Judd, F. B. Van Cleve, R. M. Thom, K. E. Buenau, et al. 2011. *Macroalgae analysis a national GIS-based analysis of macroalgae production potential summary report and project plan*. Richland, WA: Pacific Northwest National Laboratory. PNNL-21087.

Silverman-Roati, K., R.M. Webb, and M.B. Gerrard. 2021. *Removing carbon dioxide through seaweed cultivation: legal challenges and opportunities*. New York: Sabin Center for Climate Change Law.

Vijn S., D.P. Compart, N. Dutta, A. Foukis, M. Hess, A.N. Hristov, K.F. Kalscheur, E. Kebreab, S.V. Nuzhdin, N.N. Price, and Y. Sun. 2020. "Key considerations for the use of seaweed to reduce enteric methane emissions from cattle." *Frontiers in Veterinary Science* 7: 1135.

Wasson, D.E., C. Yarish, and A.N. Hristov. 2022. "Enteric methane mitigation through Asparagopsis taxiformis supplementation and potential algal alternatives." *Frontiers in Animal Science* 3: 999338.

7.3 CO_2 Emissions from Stationary Sources

Alex Badgett,[1] Gregory Cooney,[2] Jeffrey Hoffmann,[2] and Anelia Milbrandt[1]

[1] National Renewable Energy Laboratory

[2] U.S. Department of Energy Office of Fossil Energy and Carbon Management

Suggested citation: Badgett, A., G. Cooney, J. Hoffmann, and A. Milbrandt. 2024. "Chapter 7.3: CO_2 Emissions from Stationary Sources." In *2023 Billion-Ton Report*. M. H. Langholtz (Lead). Oak Ridge, TN: Oak Ridge National Laboratory. doi: 10.23720/BT2023/2316177.

7.3.1 Introduction

According to the EPA, the United States emitted about 5,547 million U.S. tons of direct CO_2 in 2022, resulting from stationary[5] and small mobile sources across economic sectors such as transportation, industry, and power generation (EPA 2022b). Stationary sources, defined as "any building, structure, facility, or installation that emits or may emit any regulated air pollutant or any pollutant listed under section 112(b) of the Clean Air Act" (Code of Federal Regulations 2016), represent a large portion (49%) of total CO_2 emissions. Most of these stationary sources currently emit CO_2 and other pollutants into the atmosphere, contributing to local air pollution and climate change (Zamuda et al. 2018). Capture of CO_2 emissions from these facilities for conversion into valuable products (including organic chemicals and transportation fuels) is an emerging opportunity that could support decarbonization across multiple sectors (Badgett, Feise, and Star 2022).

CO_2 emissions can be divided into biogenic and non-biogenic. Biogenic CO_2 emissions are defined by the EPA as those "related to the natural carbon cycle, as well as those resulting from the harvest, combustion, digestion, fermentation, decomposition, or processing of biologically based materials" (EPA 2017). In other words, biogenic CO_2 represents CO_2 that was previously sequestered from the atmosphere via plant growth. According to BETO, CO_2 emissions from ethanol plants, food and beverage operations, pulp and paper mills, dedicated biomass power plants, landfills, wastewater treatment plants, and manure management processes are considered biogenic CO_2 emissions, while non-biogenic CO_2 emissions are those resulting from the combustion of fossil fuels and other non-combustion processes (BETO 2017). For example, coal and natural gas power plants, cement manufacturing, oil and gas extraction, and many other industries emit non-biogenic CO_2. BETO is required to focus on CO_2 emissions acted on by some biological process; therefore, non-biogenic sources of CO_2 must go through a biological conversion process to be of interest to BETO (BETO 2017). The same condition does not apply

[5] Large sources of CO_2 can be referred to as "point" or "stationary" sources. In this section we distinguish between these labels at a facility level, where "stationary source" refers to a single location that emits CO_2 and "point source" refers to a specific stream of CO_2 at a stationary source, of which there can be multiple. For example, at an ethanol production facility there could be one point source of CO_2 from fermentation processes with additional on-site point sources from other processes such as natural gas combustion for process heat. Please see the appendix for further discussion.

to biogenic sources—they can go through either biological or thermochemical conversion and still be of interest to BETO (BETO 2017).

The intent for this section is to provide a high-level assessment of the potential for CO_2 captured from stationary sources to serve as a feedstock for biological-mediated processes that create carbon-based products. This section provides a CO_2 supply curve that illustrates the estimated cost of capture ($/ton) across a wide range of stationary-source categories along with county-level mapped inventories of annual (2022) CO_2 emissions for CONUS drawn from publicly available datasets. Some industries (e.g., ethanol and ammonia production) have process exhaust streams that are nearly pure in terms of CO_2 purity, and estimated cost of capture is more economically feasible than lower-purity sources. Given the comparatively lower cost, capture from sources that exhaust high-purity CO_2 is considered to be an opportunity of interest to BETO, and this section includes a closer look at the quantities and costs for this category. Non-CO_2 GHGs emitted from stationary sources such as methane, oxides, or fluorinated GHGs are not considered here.

7.3.2 CO_2 from Stationary Sources

Stationary sources of CO_2 arise from a wide range of industrial and commercial activities, and their characteristics can vary between facilities in terms of CO_2 purity, the type and percentage of any trace contaminants, and the temperature and pressure of emissions (EPA 2022a). Based on EPA's Greenhouse Gas Reporting Program (GHGRP) data, it is estimated that 2,724 million tons of CO_2 were emitted by stationary sources in 2022 (EPA 2022b). About 95% (2,584 million tons) comes from non-biogenic sources, and the remaining 5% (141 million tons) is from biogenic sources. Figure 7.27 illustrates the geographic distribution of total (biogenic and non-biogenic) CO_2 emissions from stationary sources by county.

The availability and cost of CO_2 captured from a stationary source is highly dependent on the nature of the process generating the CO_2, the scale of the source, the CO_2 capture technology, and the required properties (e.g., pressure, temperature, purity) of the CO_2 at the plant gate. Figure 7.28 shows an estimated supply curve for a range of CO_2 stationary sources and estimated cost of CO_2 capture based on datasets from the Office of Fossil Energy and Carbon Management's National Energy Technology Laboratory (NETL). Capture cost estimates provided here are based on capture technologies considered commercial or near-commercial for the specific applications. CO_2 capture systems for high-purity processes rely primarily on compression and dehydration of the already nearly pure CO_2 exhaust stream. CO_2 capture systems for low-purity streams rely primarily on solvent-based post-combustion capture technology followed by compression and dehydration of the captured CO_2 stream. Industrial facilities can vary in complexity, with some facilities limited to a single, large stationary source, while others can have multiple point sources of varying size and exhaust stream properties including total CO_2 purity and different ranges of impurities.

The estimated cost of capture reported here assumes supercritical CO_2 delivered at the fence line with a design purity suitable for pipeline transport. Examples of design considerations that could

lead to higher or lower costs are provided here but are outside the scope of this analysis. The pipeline purity specifications assumed for the costs presented here have limited consideration for trace constituents and may exclude impurities of concern for biological conversion processes.

Additional purification may be required to make the CO_2 stream a suitable feedstock for biological conversion processes. Any additional purification will likely result in increased cost of the CO_2 feedstock. The estimated capture costs also exclude transport beyond the fence line, which may be a reasonable assumption if the conversion process is located on-site. Any transport and storage needs will also lead to additional costs. Cost savings may be realized through reduction in capital and operating costs if the CO_2 can be delivered at the fence line at lower pressure than the baseline assumption.

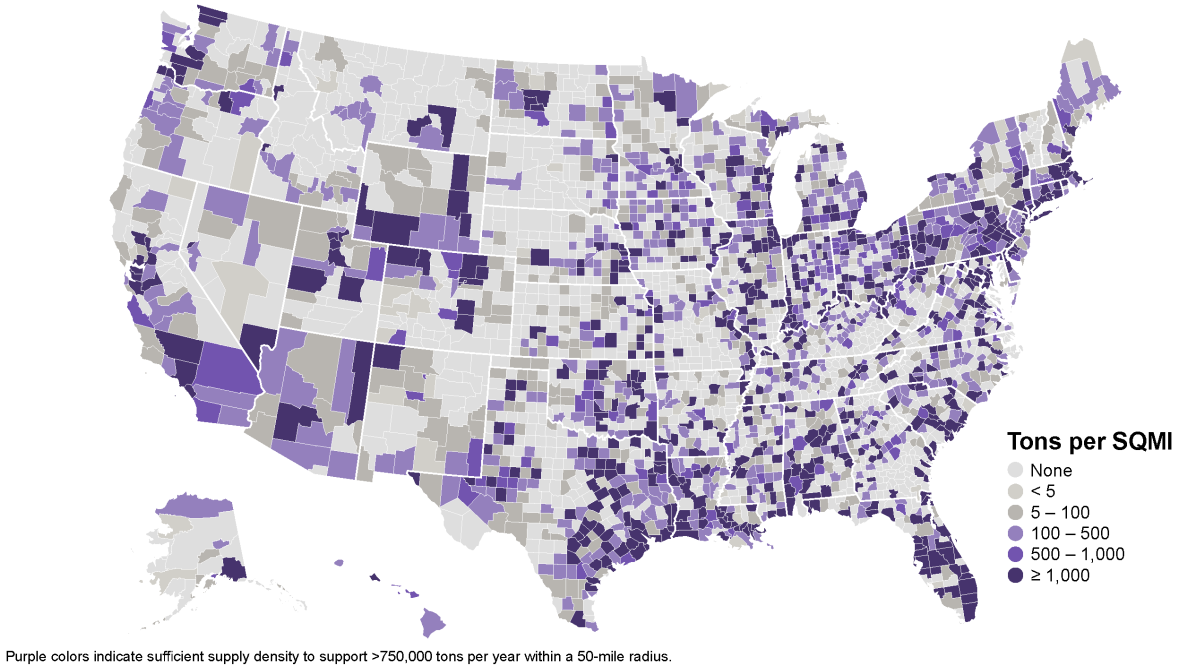

Figure 7.27. Total CO_2 emissions from stationary sources aggregated to the county level. Data adapted from the EPA's GHGRP (EPA 2022a). Please see the appendix for further discussion on how this dataset was created.

The greatest amounts of CO_2 are emitted in the Mountain West, Gulf Coast, and East Coast (Figure 7.27). The largest stationary sources of CO_2 considered here are from combustion-based processes such as coal- and natural-gas-fired power plants and large-scale steel manufacturing (Figure 7.28). While these facilities emit the largest amounts of CO_2, the CO_2 purity in flue gas emissions is low (<30%) and can have impurities that make capture and purification more costly (Hughes and Zoelle 2023; Schmitt et al. 2022) (Figure 7.28). Because the largest single sources of CO_2 tend to be from combustion-based processes, CO_2 captured from these sources might not be available at the lowest costs. Moreover, emitting facilities are often spatially dispersed and may not be in close proximity to demand for CO_2-based products. Cost associated with transport from the point of capture to end use, as well as additional purification (if needed), are not

included in the cost estimates provided here and would be adders to the final "delivered price." How and where CO_2 utilization systems are deployed will depend on the particular product being manufactured, potential additive costs for transporting either CO_2 or CO_2-based products, and other market factors that are beyond the scope of this work.

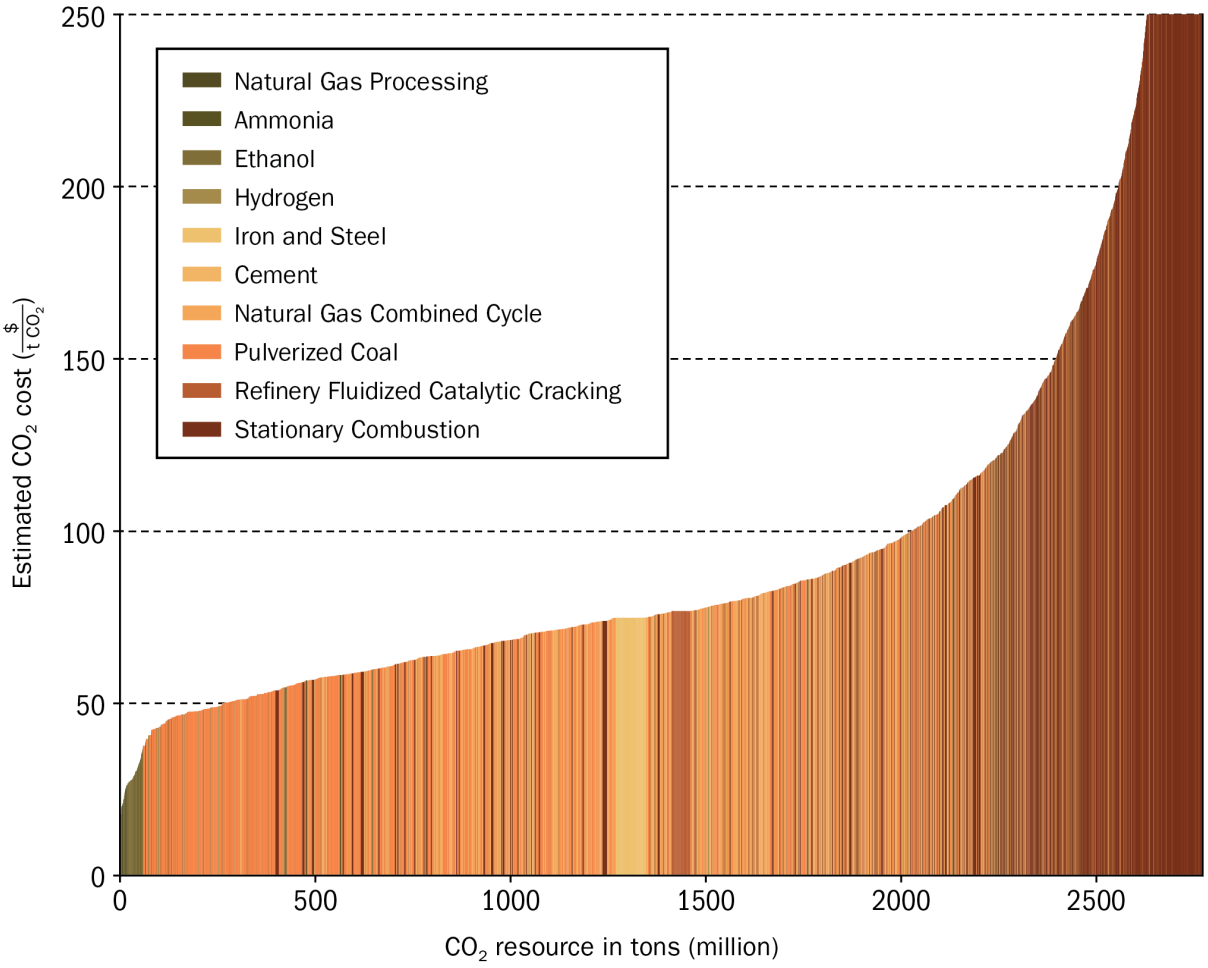

Figure 7.28. Subset of total CO_2 resource by facility category for stationary source and estimated cost of CO_2 capture and purification. Figure using data from NETL and the Office of Fossil Energy and Carbon Management (NETL 2023; Fahs et al. 2023; Schmitt et al. 2023). Please see the appendix for further information.

Variability also exists in total resource estimates between datasets and by year. Total CO_2 emitted from stationary sources (Figure 7.27) uses EPA datasets from 2022, while data shown in Figures 7.28, 7.29, and 7.30 are based on 2021 datasets. While the year-by-year variations in CO_2 streams likely influence the total amounts in these datasets slightly, explicitly quantifying and comparing these differences is beyond the scope of the nationwide resource analysis discussed in this section. Annual changes in total potential CO_2 supply can result from facility-level changes (e.g., operation, equipment improvements and process design, feedstock input changes) as well as demand for end-use products (i.e., decrease in reliance on electricity generated from fossil fuels would decrease sector emissions, while increase in demand for

domestically produced steel or cement would increase associated sector emissions). For example, in 2019 the National Petroleum Council estimated approximately 2,866 million tons of CO_2 from stationary sources (National Petroleum Council 2019), while this 2022 analysis estimates about 2,724 million tons of CO_2. While fossil-fueled (coal and natural gas) power plants compose the largest single stationary source categories of CO_2 currently and may be required to consider CO_2 capture under proposed regulations (EPA 2023), ongoing efforts to decarbonize the electric power sector may result in the closure of high-emitting facilities and would likely reduce the respective total amount of CO_2 available for capture, conversion, and use. How large-scale CO_2 markets might respond to such supply dynamics is uncertain and will depend on factors like demand profiles for CO_2-based products, competing technology pathways, and other market forces.

7.3.3 Opportunities and Market Outlook

Stationary sources from processes that produce high-purity CO_2 exhaust streams (e.g., ethanol and ammonia production plants) are less expensive to capture and purify compared to exhaust gases with low CO_2 purity, making them more attractive feedstocks. These sources and existing applications for high-purity CO_2 streams are discussed in detail in this section. High-purity CO_2 stationary sources are generally associated with agriculture, and are therefore predominantly sited in the central United States (Figure 7.29), and are the primary driving force for the lower CO_2 capture costs shown in these areas (Figure 7.30). This analysis does not focus on capture and purification technologies beyond the high-level discussion and data provided in this section and its appendix, but readers should note that the cost of capture and purification of CO_2 depends on the state of these technologies. Advances in process efficiency, novel capture technologies, and integrated capture and conversion systems could shift these costs and therefore CO_2 market development.

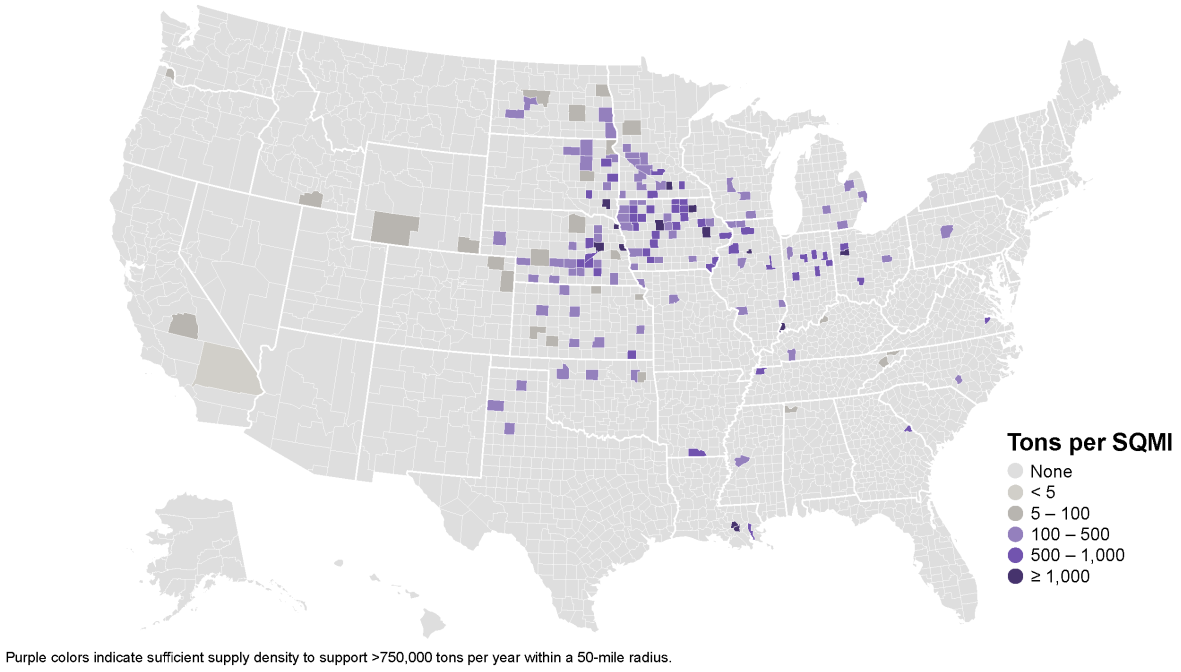

Figure 7.29. Estimated supply of high-purity CO_2 for ethanol and ammonia production facilities. These supply estimates exclude high-purity CO_2 already captured at operating facilities. See the appendix for additional detail.

Use of high-purity streams of CO_2 from ethanol and ammonia stationary sources is viewed as the most amenable for near-term deployment of biologically mediated CO_2 conversion processes. As discussed further in the appendix, some of these facilities are already capturing the high-purity CO_2 and utilizing it on-site (ammonia conversion to urea) or selling into the merchant market. However, these high-purity sources represent only a portion of total CO_2 emitted from stationary sources annually (the selected resources provided here represent about 47.2 million tons, or 2% of total stationary-source CO_2 emissions reported by the EPA). If demand from large-scale CO_2 utilization technologies exceeds the available high-purity resources, capture from additional stationary sources will likely be from processes producing lower-purity CO_2 streams and higher costs of capture.

When assessing the feasibility of capturing CO_2 from stationary sources, it is important to evaluate the site-specific aspects of CO_2 availability and process-level design of the facility. Total amounts of CO_2 reported to the EPA from a single facility can encompass streams from multiple different processes and unit operations, with potential variation in the feasibility of capturing each stream. For example, ethanol and ammonia production facilities emit high-purity streams of CO_2 from specific processes but are also likely to emit lower-purity CO_2 streams from other unit operations such as natural gas combustion for process heat, among others. Moreover, configuration of the capture process can influence both the amount and purity of the product CO_2. Additional CO_2 may be produced if carbon-based fuels (fossil or biomass) are used to satisfy thermal energy requirements of the capture system. Additionally, CO_2 product purity can

vary depending on the degree and nature of treated stream impurities, as well as the characteristics of the CO_2 capture process. Lastly, purity requirements of CO_2 as a feedstock can impact the feasibility of the conversion process. Understanding the nature of the CO_2 resource at the facility level (e.g., specific proportions of high- and low-purity CO_2 streams, types and quantities of non-CO_2 impurities) and requirements of the conversion technology of interest is crucial to designing and optimizing integration of CO_2 sources with on-site conversion technologies.

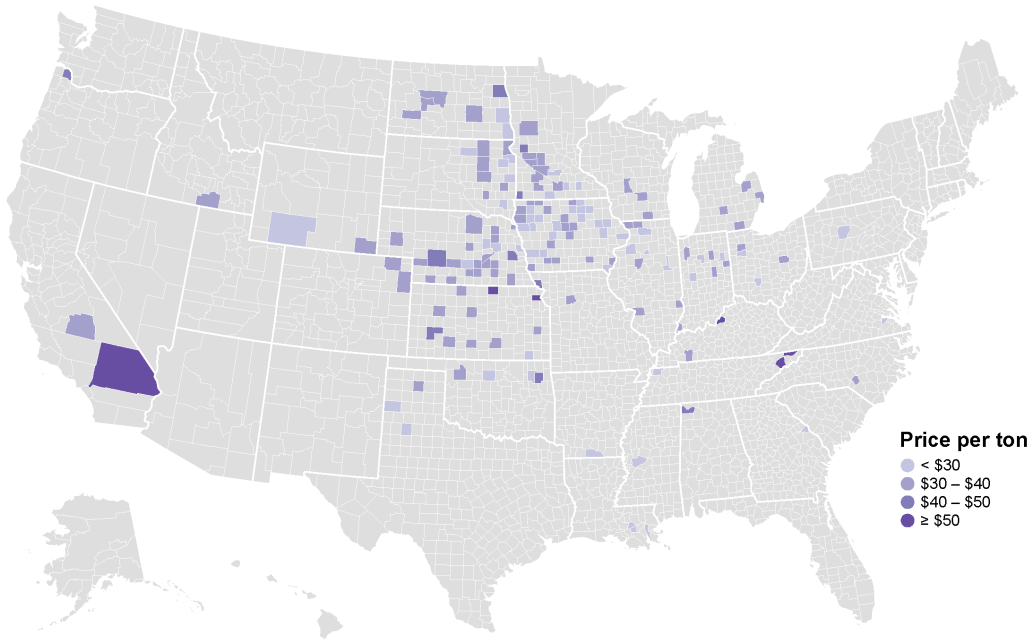

Figure 7.30. Average estimated cost of high-purity CO_2 captured from ethanol and ammonia production facilities

Markets for CO_2 are present in the United States today and consume CO_2 from existing sources at a small scale relative to total annual emissions (EPA 2022c). The total amount of CO_2 captured from industrial sources and produced from natural sources (excluding CO_2 captured and utilized on-site, such as production of urea at integrated ammonia facilities) in the United States was 52.5 million tons in 2022 (EPA 2022c). This amount represents about 1.9% of total supply from the stationary sources considered in this analysis. The majority of CO_2 emissions from stationary sources (98.1%) is released to the atmosphere and is not currently captured in a form available for utilization. As of 2022, the majority of CO_2 captured and utilized was used for enhanced oil recovery (40 million tons, or about 78%), with other consumers including food and beverage (5.5 million tons, or about 10%), pulp and paper manufacturing, and other industries (EPA 2022c). Almost 40% of this utilized CO_2 comes from the capture of emissions from industrial facilities, including ethanol plants, natural gas processing facilities, and ammonia plants, again demonstrating the favorability of leveraging the lower cost of capturing CO_2 from process streams that have high (near-pure) CO_2 purities. While the current amount of CO_2

captured and utilized is small, it is clear that the majority of this CO_2 comes from economically favorable, high-purity, stationary-source emissions (e.g., ethanol and ammonia plants).

Decarbonization efforts in industry and the power sector will also influence CO_2 availability, and a number of current incentives may act favorably for the deployment of respective capture technologies and non-carbon alternatives, such as greater reliance on renewable resources for power generation and hydrogen produced as a replacement for fossil-fuel-intensive industries (e.g., steel manufacturing). Over the long term, structural changes of energy-intensive industries as a means to transition to net-zero technologies may lead to significant reduction and possibly elimination of existing industries considered as potential CO_2 resources. Recent analysis (Zhou et al. 2023) suggests that existing CO_2 stationary sources could reduce in the future as fossil-fuel-based power generation and industrial processes shift and move toward decarbonization, and other stationary sources such as cement, ethanol, and ammonia production continue to operate and might represent a larger share of CO_2 supply. However, other stationary sources of CO_2 could emerge from bioenergy processes in the future, again shifting the supply of CO_2 available and likely impacting prices for this stream.

Precedent for shifts in these future markets can be seen in the development of RNG from organic sources, valorizing these emissions and impacting the value of gases that might otherwise be viewed as wastes. It is important to note that this trajectory is just one possibility in a future that could change depending on numerous technical, economic, and regulatory uncertainties. Depending on the future market demand for CO_2-based fuels and products and the current state of direct air capture technologies, direct air capture could also provide atmospheric CO_2. Understanding the dynamics between CO_2 stationary sources, decarbonization efforts, and opportunities to deploy CO_2 removal technologies such as direct air capture is crucial for processes aiming to produce CO_2-based fuels and products.

It is reasonable to expect that as markets for CO_2 emissions develop, demand will increase and technology advances could impact supply dynamics and resource prices in ways that cannot be easily projected and are not contemplated in this analysis. As such, future potential end uses could compete with bioenergy-specific CO_2 utilization pathways and should be considered in subsequent resource and market analyses. Using modeling capabilities developed for the microalgae portion of this report, we considered potential competitive use estimates for CO_2 emissions in the case that microalgae pathways utilize stationary-source emissions. Under deployment scenarios for microalgae pathways, we estimate that a range of 5%–10% of total CO_2 emissions from stationary sources could be used for conversion. For further information and discussion on microalgae utilization and modeling, please refer to Section 7.1.

References

Badgett, Alex, Alison Feise, and Andrew Star. 2022. “Optimizing Utilization of Point Source and Atmospheric Carbon Dioxide as a Feedstock in Electrochemical CO2 Reduction." Article No. 104270.

Bioenergy Technologies Office (BETO). 2017. *Biofuels and Bioproducts from Wet and Gaseous Waste Streams: Challenges and Opportunities*. Washington, D.C.: BETO. energy.gov/sites/default/files/2017/09/f36/biofuels_and_bioproducts_from_wet_and_gaseous_waste_streams_full_report.pdf.

Code of Federal Regulations. 2016. "40 CFR 70.2 -- Definitions." ecfr.gov/current/title-40/part-70/section-70.2.

Fahs, Ramsey, Rory Jacobson, Andrew Gilbert, Dan Yawitz, Catherine Clark, Jill Capotosto, Colin Cunliff, Brandon McMurty, and Lee Uisung. 2023. *Pathways to Commercial Liftoff: Carbon Management*. Washington, D.C.: DOE. liftoff.energy.gov/wp-content/uploads/2023/06/20230424-Liftoff-Carbon-Management-vPUB_update3.pdf.

Hughes, Sydney, and Alexander Zoelle. 2023. *Cost of Capturing CO_2 from Industrial Sources*. DOE/NETL-2023/3907. National Energy Technology Laboratory. netl.doe.gov/projects/files/CostofCapturingCO2fromIndustrialSources_033123.pdf.

National Energy Technology Laboratory (NETL). 2023. "Industrial CO2 Capture Retrofit Database (IND CCRD) Public Rev 62." Dec. 19, 2023. National Energy Technology Laboratory. netl.doe.gov/ea/CCRS.

National Petroleum Council. 2019. "Meeting the Dual Challenge: A Roadmap to At-Scale Deployment of Carbon Capture, Use, and Storage." dualchallenge.npc.org/downloads.php.

Schmitt, Tommy, Sally Homsy, Hari Mantripragada, Mark Woods, Hannah Hoffman, Travis Shultz, Timothy Fout, and Gregory Hackett. 2023. *Cost and Performance of Retrofitting NGCC Units for Carbon Capture - Revision 3*. DOE/NETL-2023/3848. National Energy Technology Laboratory. netl.doe.gov/projects/files/CostandPerformanceofRetrofittingNGCCUnitsforCarbonCaptureRevision3_053123.pdf.

Schmitt, Tommy, Sarah Leptinsky, Marc Turner, Alexander Zoelle, Charles W. White, Sydney Hughes, Sally Homsy, et al. 2022. *Cost and Performance Baseline for Fossil Energy Plants Volume 1: Bituminous Coal and Natural Gas to Electricity*. DOE/NETL-2023/4320. National Energy Technology Laboratory. netl.doe.gov/energy-analysis/details?id=e818549c-a565-4cbc-94db-442a1c2a70a9.

U.S. Environmental Protection Agency (EPA). 2017. "Carbon Dioxide Emissions Associated with Bioenergy and Other Biogenic Sources." Overviews and Factsheets. 19january2017snapshot.epa.gov/climatechange/carbon-dioxide-emissions-associated-bioenergy-and-other-biogenic-sources.

———. 2022a. "2022 Data Summary Spreadsheets." Overviews and Factsheets. epa.gov/ghgreporting/data-sets.

———. 2022b. "Greenhouse Gas Inventory Data Explorer." cfpub.epa.gov/ghgdata/inventoryexplorer/#iallsectors/allsectors/carbondioxide/inventsect/current.

———. 2022c. "Supply, Underground Injection, and Geologic Sequestration of Carbon Dioxide." Other Policies and Guidance. epa.gov/ghgreporting/supply-underground-injection-and-geologic-sequestration-carbon-dioxide.

———. 2023. “New Source Performance Standards for Greenhouse Gas Emissions From New, Modified, and Reconstructed Fossil Fuel-Fired Electric Generating Units; Emission Guidelines for Greenhouse Gas Emissions From Existing Fossil Fuel-Fired Electric Generating Units; and Repeal of the Affordable Clean Energy Rule.” *Federal Register* 88 FR 33240. May 23, 2023. federalregister.gov/documents/2023/05/23/2023-10141/new-source-performance-standards-for-greenhouse-gas-emissions-from-new-modified-and-reconstructed.

Zamuda, C., D.E. Bilello, G. Conzelmann, E. Mecray, A. Satsangi, V. Tidwell, and B.J. Walker. 2018. *Impacts, Risks, and Adaptation in the United States: Fourth National Climate Assessment, Volume II*. D.R. Reidmiller, C.W. Avery, D. Easterling, K. Kunkel, K.L.M. Lewis, T.K. Maycock, and B.C. Stewart (Eds.). Vol. 2. Washington, D.C.: U.S. Global Change Research Program. doi.org/10.7930/NCA4.2018.CH4.

Zhou, Ella, Amgad Elgowainy, Andre Fernades Tomon Avelino, Hoon Baek, Wesley Cole, Garvin Heath, Yijin Li, Weijia Liu, Pingping Sun, and Jiazi Zhang. 2023. “Markets, Resources, and Environmental and Energy Justice (MarkeRs-EEJ).” Presented at the DOE Bioenergy Technologies Office (BETO) 2023 Project Peer Review, Denver, CO. energy.gov/sites/default/files/2023-04/beto-03-project-peer-review-c02-apr-2023-zhou.pdf.